

MS106

Complex Analysis and PDEs

Multi-Scale Conformal Maps for Singular Interfaces in Free Boundary Problems
Shankar C. Venkataramani, University of Arizona.

Conformal Mapping Technique for a Supercavitating Flow Around a Wedge Or a Hydrofoil
Anna Zemlyanova, Kansas State University.

Weak Solutions for Integrable Free-Boundary Dynamics in Two Dimensions
Razvan Teodorescu, University of South Florida.

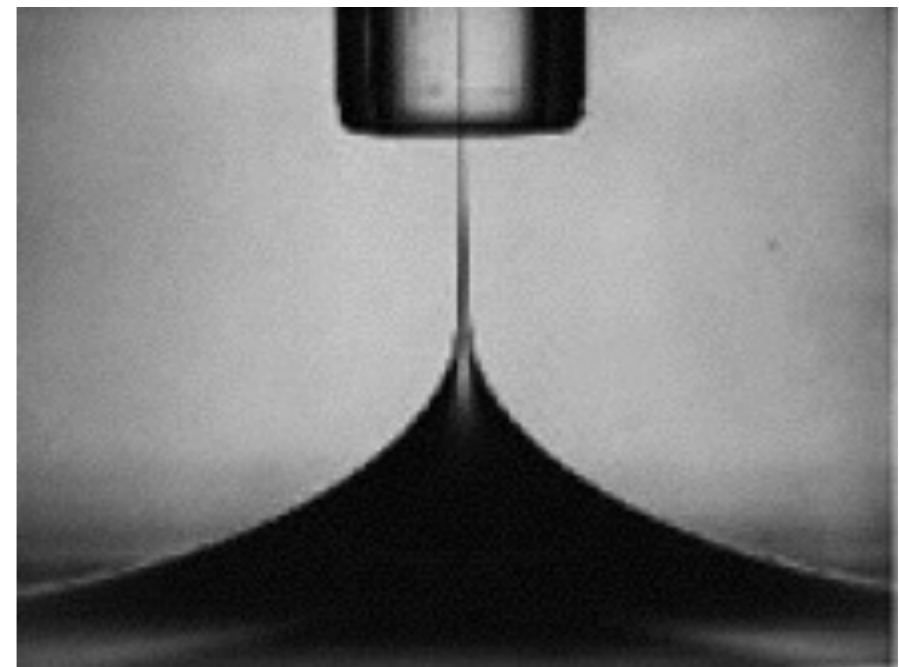
Burgers Equation in the Complex Plane and Random Matrix Theory
Govind Menon, Brown University.

Multi-Scale Conformal Maps for Singular Interfaces in Free Boundary Problems

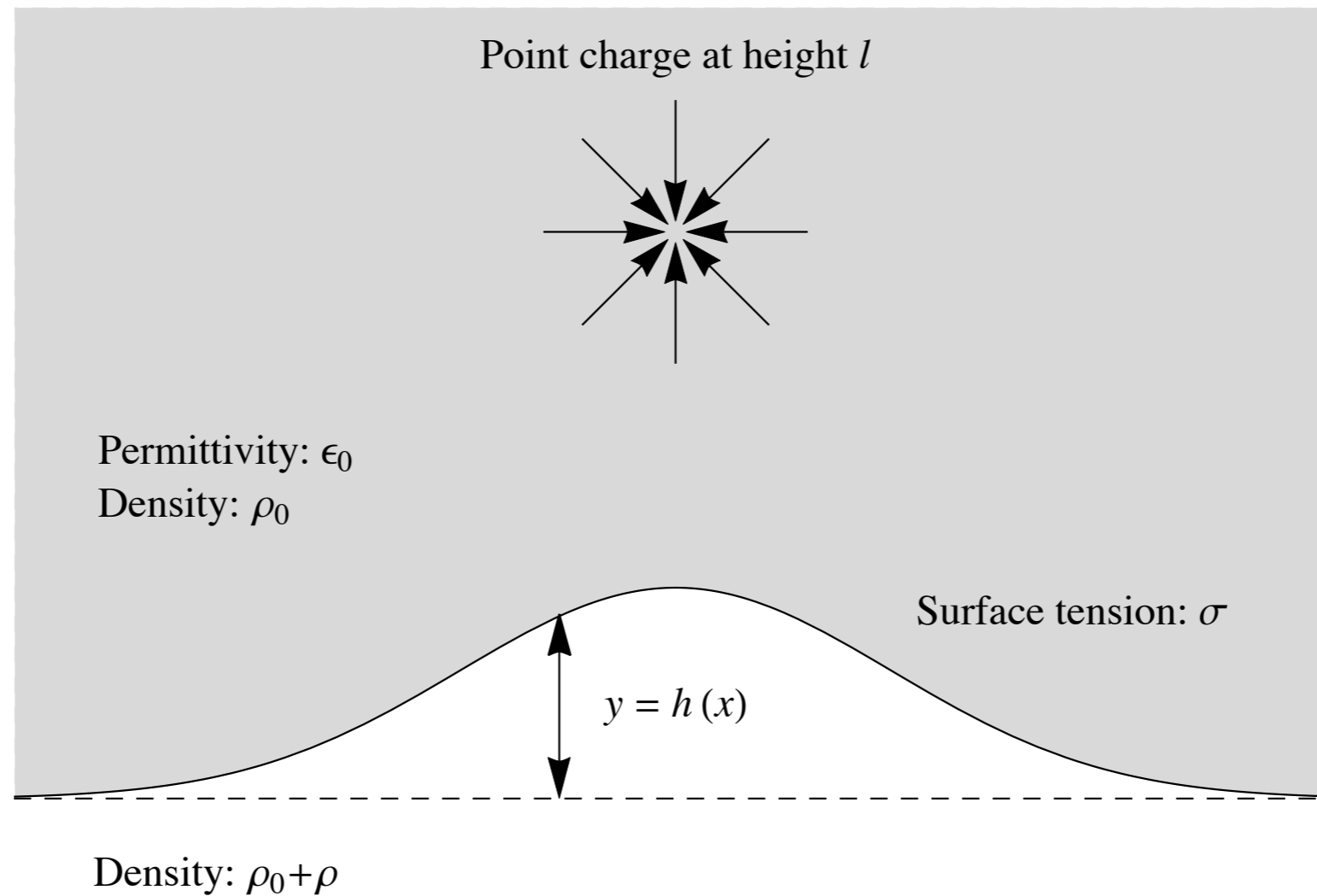
Stuart Kent

Shankar Venkataramani

University of Arizona



The Model



$$-\sigma \kappa(x) + \rho g h(x) = \frac{\epsilon_0}{2} \left(\frac{\partial \phi}{\partial n} \right)^2 \quad \text{for } x \in (-\infty, \infty).$$

Governing equations

(Dimensionless) **Governing Equations:**

$$\underbrace{\frac{h_{xx}(x)}{(1 + h_x^2(x))^{3/2}}}_{\text{elastic tension}} - \underbrace{h(x)}_{\text{gravity}} = \underbrace{- (\nabla\phi(x, h) \cdot n(x))^2}_{\text{electrostatic pressure}} \text{ for } x \in (-\infty, \infty)$$

ϕ : dimensionless electric potential above the interface.

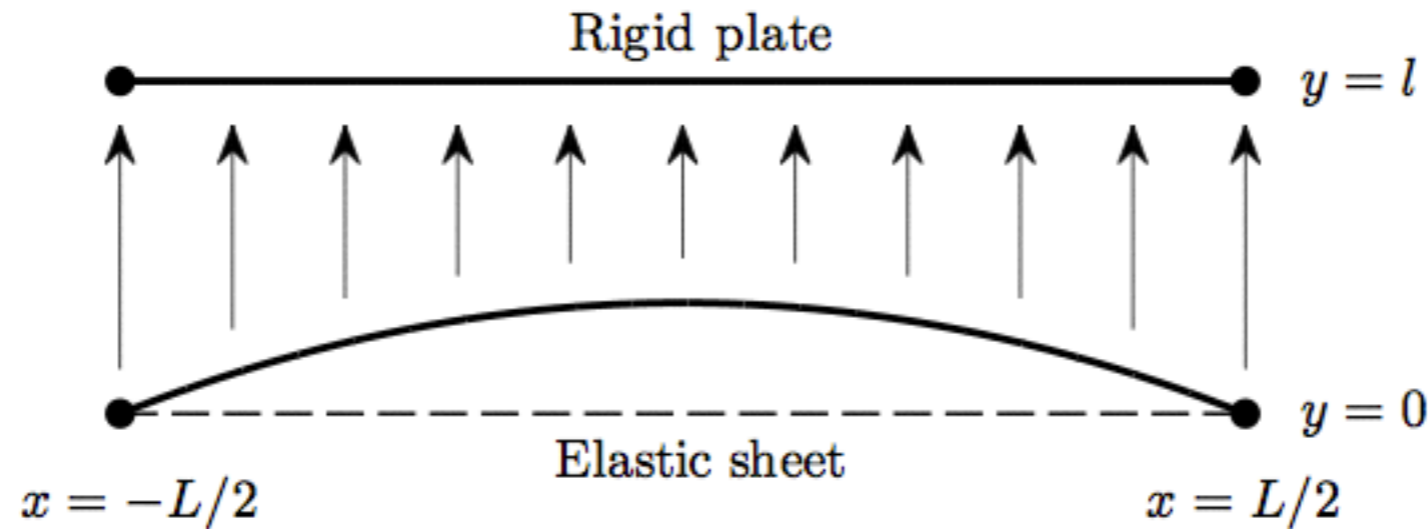
n : upward unit normal to the interface.

$$\nabla^2\phi(x, y) = -q\delta(x, y - l) \text{ in } \{h(x) < y : x \in (-\infty, \infty)\}$$

$$\phi(x, h(x)) = 0 \text{ for } x \in (-\infty, \infty)$$

$$h(x) \rightarrow 0 \text{ as } x \rightarrow \pm\infty.$$

MEMS devices



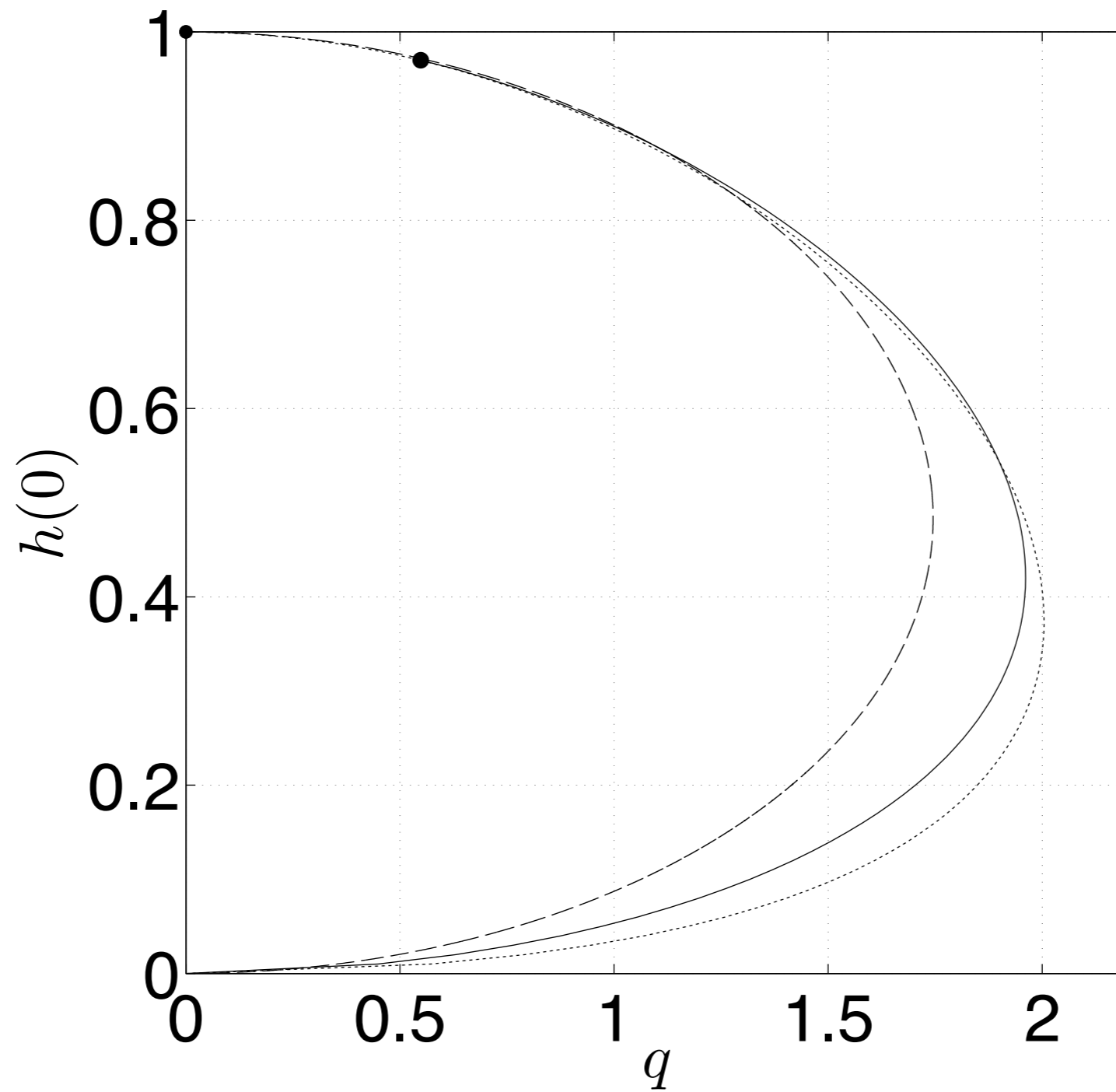
Potential difference is applied between plate and conducting sheet.

Sheet deflects towards the plate and reaches equilibrium for relatively low potential difference.

Beyond a critical potential difference, no equilibrium exists (*pull-in instability*).

Pelesko, Lindsay, Moulton, Brubaker, Lega, ...

Schematic bifurcation diagram



Continuation method

Conformal maps and the pullback of harmonic functions

Definition

A function $\mathbb{F}(w)$ defined on $\Omega \subset \mathbb{C}$ is called *conformal* at $w_0 \in \Omega$ if it preserves angles in a neighborhood of w_0 .

Theorem

Let $\hat{\phi}$ solve Laplace's equation in $\Omega \subset \mathbb{C}$, and let $\mathbb{F} : \Omega \rightarrow \Omega_0$ defined by $z = \mathbb{F}(w) = x(u, v) + iy(u, v)$ be conformal in Ω . Then the function ϕ defined by $\phi(x, y) = \hat{\phi}(u, v)$ solves Laplace's equation in Ω_0 .

Conformal mapping

Conformal maps may be identified with one-to-one analytic functions.

Theorem

A map $F : \Omega \rightarrow \mathbb{C}$ defined on a domain $\Omega \subset \mathbb{C}$ is conformal if and only if the function F is analytic and has non-vanishing derivative ($F' \neq 0$) everywhere on Ω .

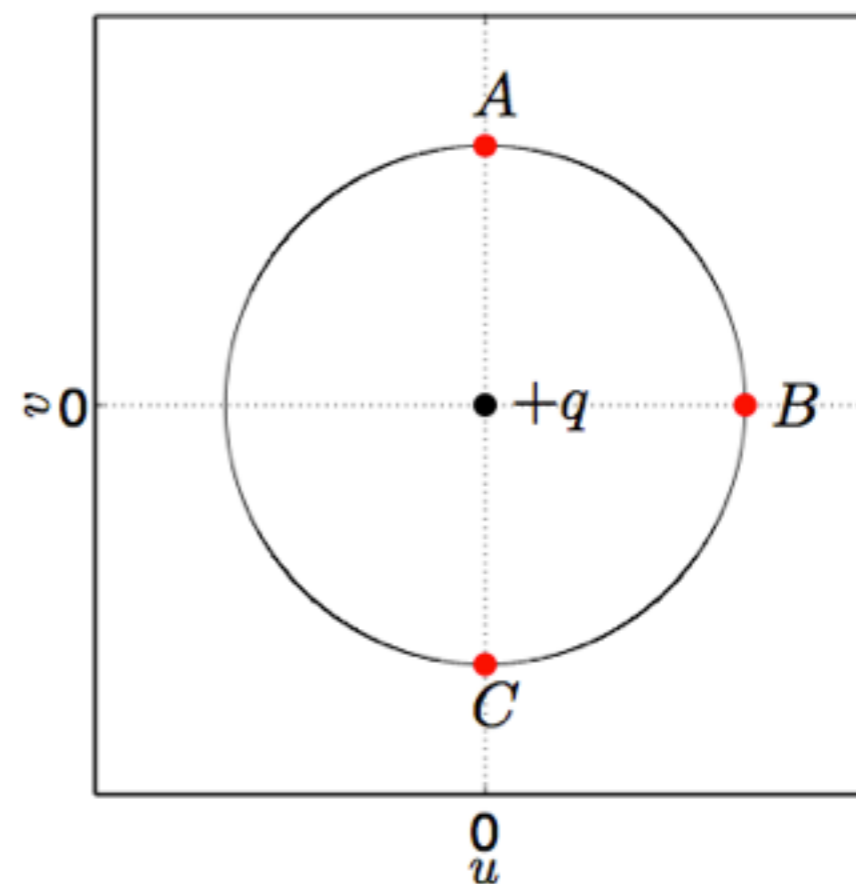
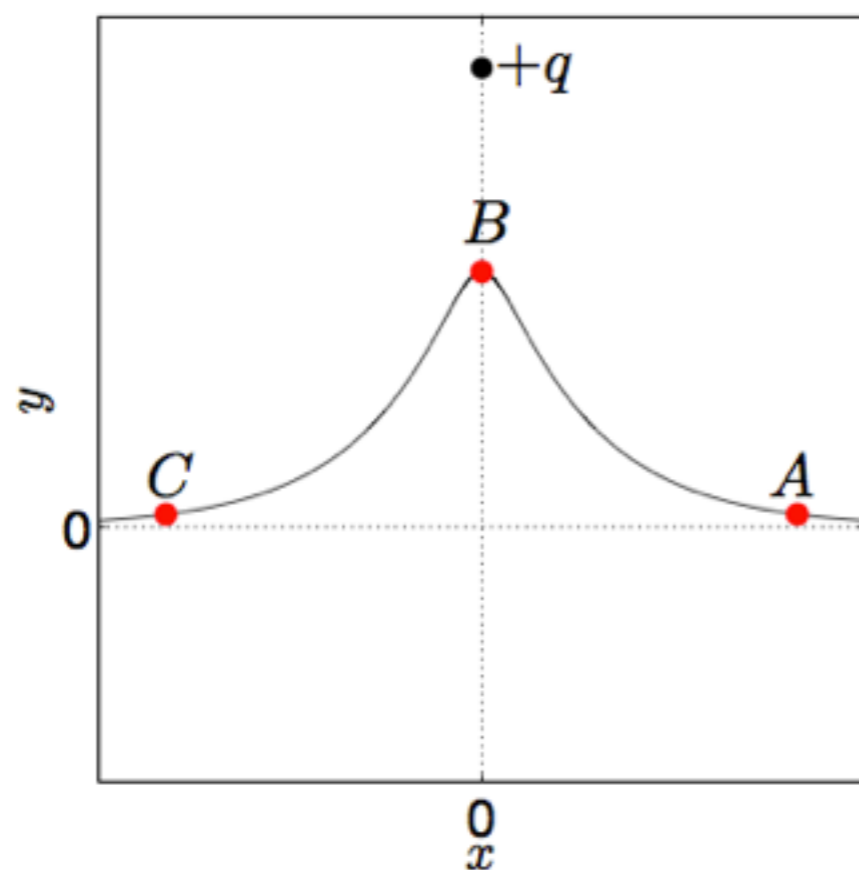
Conformal maps provide a rich class of candidate profiles

Theorem (Riemann mapping theorem)

If Ω is a non-empty simply-connected proper open subset of \mathbb{C} , then there exists a bijective analytic function f from Ω onto the unit disc $\mathbb{D} = \{w : |w| < 1\}$.

Mapping the domain

Reduce from complicated domain to simpler domain $\mathbb{D} \subset \mathbb{C}$:



Solution for the electrostatic potential on the disk with point charge at the origin:

$$\hat{\phi}(w) = -\frac{q}{2\pi} \log |w|$$

Complex variable formulation I

We recast the governing equations in terms of $\zeta(\theta) = F(e^{i\theta}) = x(\theta) + ih(\theta)$.

Gravitational term:

$$h(x(\theta)) = \text{Im}(\zeta(\theta)).$$

Elastic term:

$$\begin{aligned}\kappa(x(\theta)) &= \frac{x_\theta(\theta)h_{\theta\theta}(\theta) - h_\theta(\theta)x_{\theta\theta}(\theta)}{(x_\theta^2(\theta) + h_\theta^2(\theta))^{3/2}}, \\ &= \frac{\text{Im}(\zeta_{\theta\theta}(\theta)\overline{\zeta_\theta(\theta)})}{|\zeta_\theta(\theta)|^3}.\end{aligned}$$

Complex variable formulation II

Electrostatic term:

Induced pressure $|\nabla\hat{\phi}|^2$ on $\partial\mathbb{D}$ has uniform magnitude $(q/2\pi)^2$.

Equipotentials are separated by a factor of $|\mathbb{F}_w(e^{i\theta})| = |\zeta_\theta(\theta)|$ near $\zeta(\theta)$.

So electrostatic term is

$$|\nabla\phi(x(\theta), h(\theta)) \cdot n|^2 = \left(\frac{q}{2\pi|\zeta_\theta(\theta)|} \right)^2.$$

Governing equations

$$-\frac{\operatorname{Im}(\zeta_{\theta\theta}(\theta)\bar{\zeta}_{\theta}(\theta))}{|\zeta_{\theta}(\theta)|^3} + \operatorname{Im}(\zeta(\theta)) = \left(\frac{q}{2\pi|\zeta_{\theta}(\theta)|}\right)^2$$

for $\theta \in (-\pi, \pi)$.

A “real” equation for a complex valued function.

Lemma

Let $\mathbb{F}(w)$ be an analytic function defined on \mathbb{D} . The real and imaginary parts of \mathbb{F} satisfy the relationship

$$\operatorname{Re}(\mathbb{F}(w)) = -\operatorname{Im}(\mathcal{H}[\mathbb{F}](w))$$

$$\operatorname{Im}(\mathbb{F}(w)) = +\operatorname{Re}(\mathcal{H}[\mathbb{F}](w))$$

on $\partial\mathbb{D}$, where \mathcal{H} is the Hilbert Transform.

The periodic Hilbert transform \mathcal{H} of a periodic function ξ is defined by

$$\mathcal{H}[\xi](\phi) = \lim_{\epsilon \rightarrow 0} \frac{1}{2\pi} \int_{\epsilon}^{\pi} \cot\left(\frac{\theta}{2}\right) [\xi(\phi - \theta) - \xi(\phi + \theta)] d\theta$$

Natural mapping between analytic functions on the closed unit disk and Fourier series:

$$\Upsilon(w) = \sum_n a_n w^n \leftrightarrow \sum_n a_n e^{in\theta} = v(\theta)$$

Since Υ is analytic at 0, it follows that

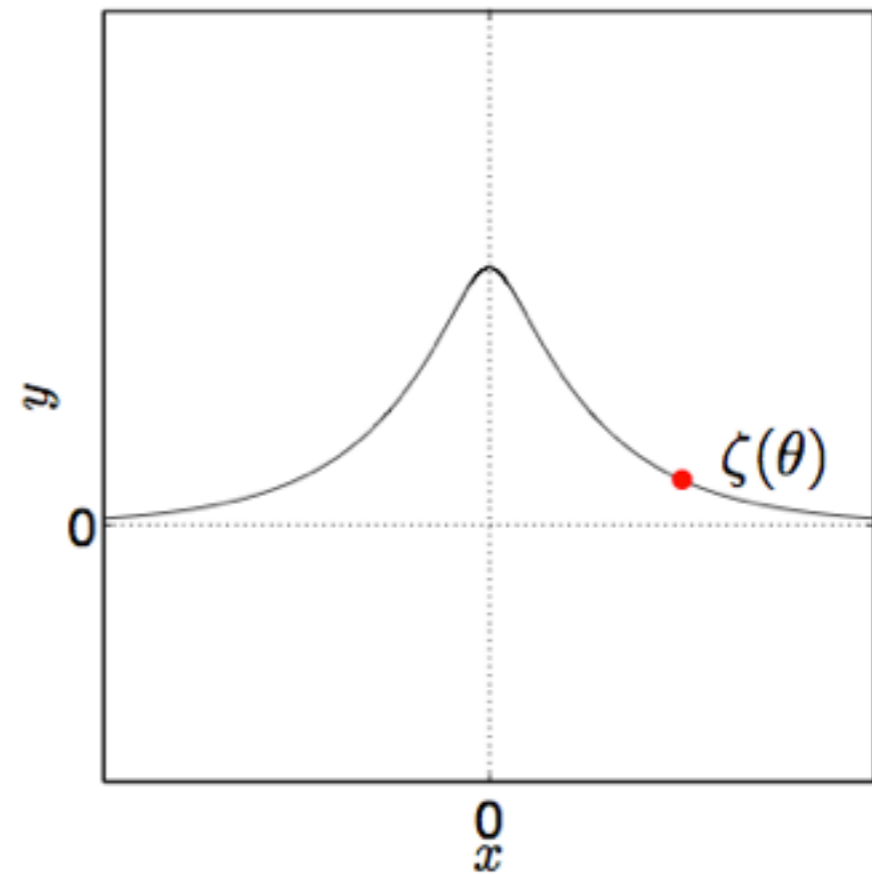
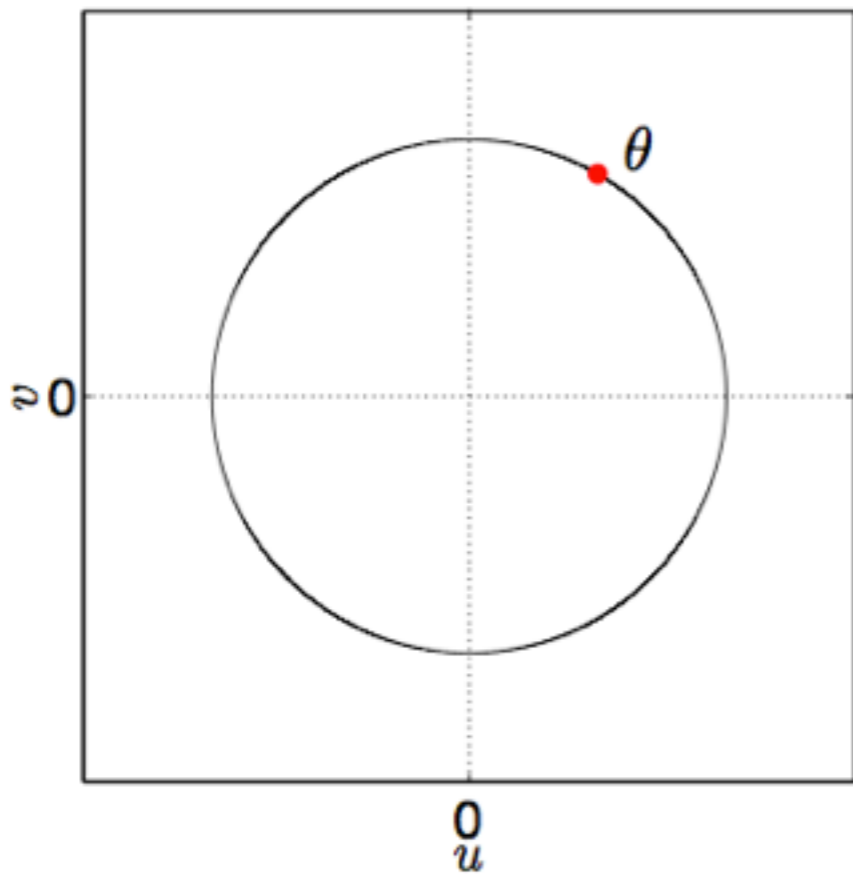
$$a_{-n} = \frac{1}{2\pi} \int_0^{2\pi} v(\theta) e^{in\theta} d\theta = 0 \text{ for } n = 1, 2, \dots \quad (1)$$

Equations are local in the **transform domain** (in terms of n), but are **nonlocal integral equations** in terms of θ .

Conformal parameterization of the interface

We write $\zeta(\theta) = x(\theta) + ih(\theta) = i\mathbb{F}(e^{i\theta})$ for $\theta \in (-\pi, \pi)$.

ζ is a parametrized representation of the candidate deflection profile in the image plane.



$$x \rightarrow \pm\infty, y \rightarrow 0 \text{ as } \theta \rightarrow \pm 1$$

No other singularities in the unit disk or its boundary.

Boundary conditions

$x \rightarrow \pm\infty, y \rightarrow 0$ as $\theta \rightarrow \pm 1$

$F(w)$ has a simple pole at $w = 1$. Consequently $(1 + w)F(w)$ is analytic on \mathbb{D} .

Representations of F :

$$\begin{aligned} F(w) &= \frac{G(w)}{1+w} \\ &= \frac{G(-1)}{1+w} + \frac{G(w) - G(-1)}{1+w} \\ &= \frac{G(-1)}{2} \frac{1-w}{1+w} + \left[\frac{G(-1)}{2} + \frac{G(w) - G(-1)}{1+w} \right] \\ &= A \frac{1-w}{1+w} + B(w) \end{aligned}$$

Conformal reformulation

$$F(w) = \alpha \frac{1-w}{1+w} + B(w)$$

$$f(\theta) = \lim_{w \rightarrow e^{i\theta}} F(w)$$

$$\zeta(\theta) = if(\theta)$$

$$\frac{q^2}{4\pi^2 |f_\theta(\theta)|^2} - \operatorname{Re}[f(\theta)] + \frac{\operatorname{Im}[f_{\theta\theta}(\theta) \overline{f_\theta(\theta)}]}{|f_\theta(\theta)|^3} = 0.$$

$$\int_0^{2\pi} (1 + e^{i\theta}) f(\theta) e^{in\theta} d\theta = 0 \text{ for } n = 1, 2, \dots$$

$$l = F(0) = \frac{1}{2\pi} \int_0^{2\pi} (1 + e^{i\theta}) f(\theta) d\theta,$$

Collocation method

$$\tilde{F}(w) = \alpha \left(\frac{1-w}{1+w} \right) + \sum_{j=0}^M \beta_j w^j.$$

$$\tilde{f}(\theta) = -i\alpha \tan \left(\frac{\theta}{2} \right) + \sum_{j=0}^M \beta_j e^{ij\theta} \text{ for } \theta \in (-\pi, \pi)$$

$\alpha, \beta_0, \beta_1, \dots, \beta_M$ are all real

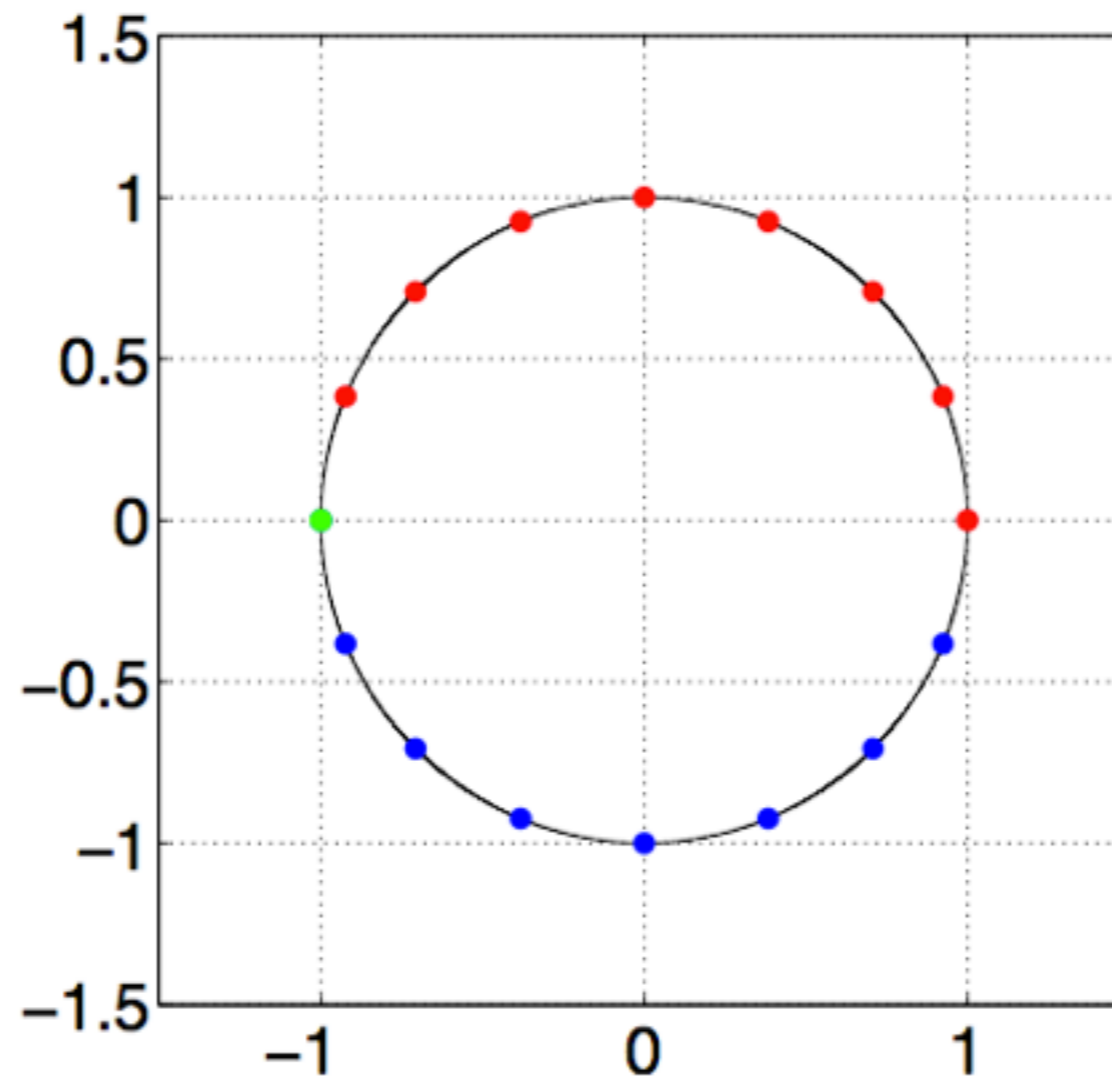
$$l = \alpha + \beta_0 \quad \sum_{j=0}^M (-1)^j \beta_j = 0$$

Residual :

$$R[\tilde{f}] \equiv \frac{q^2}{4\pi^2 |\tilde{f}_\theta(\theta)|^2} - \operatorname{Re}[\tilde{f}(\theta)] + \frac{\operatorname{Im}[\tilde{f}_{\theta\theta}(\theta) \overline{\tilde{f}_\theta(\theta)}]}{|\tilde{f}_\theta(\theta)|^3}$$

Discretization

We specify heights h_j (imaginary part of ζ) at each red node:

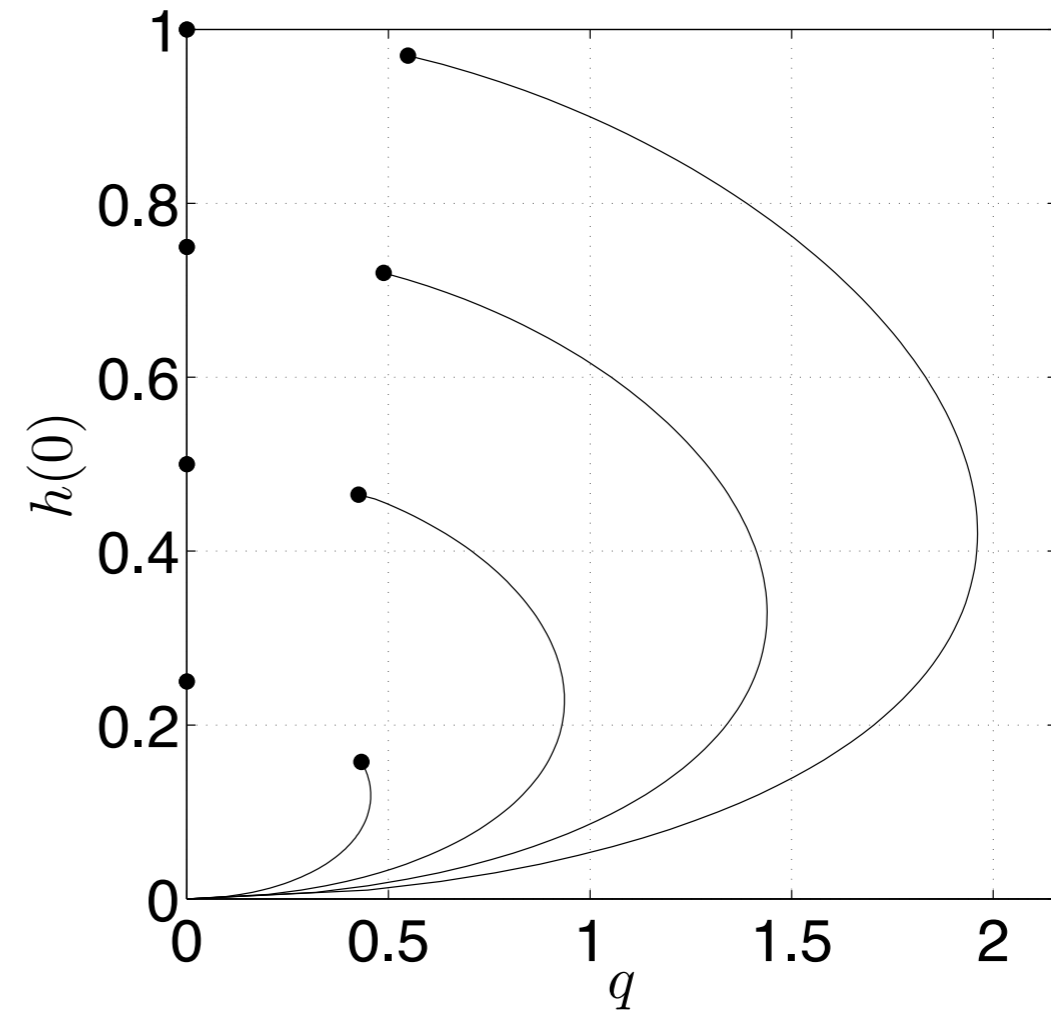
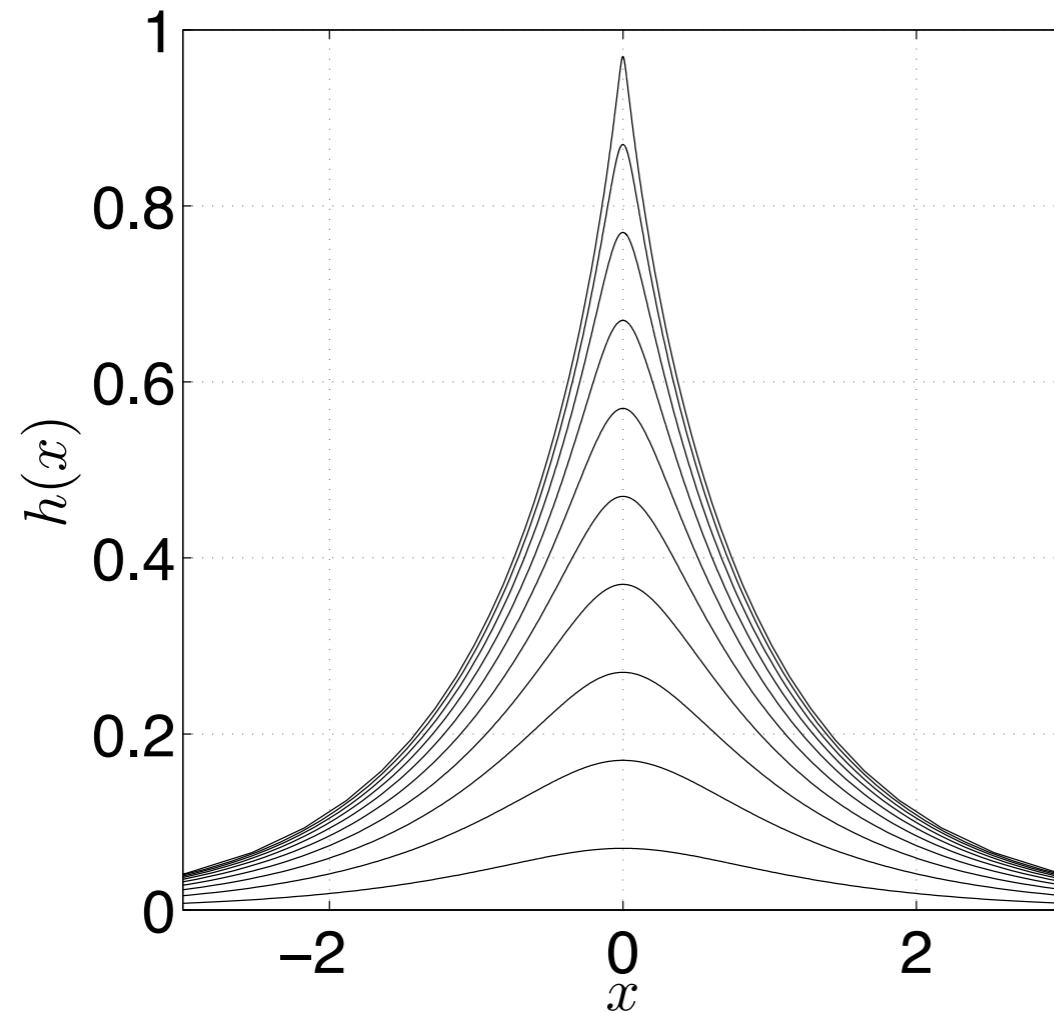


Symmetry and decay \Rightarrow heights at other nodes.

Methods of Numerical Conformal Mapping, R. Wegmann (2005)

Method is intrinsically non-adaptive!; Wilkening, 2011.

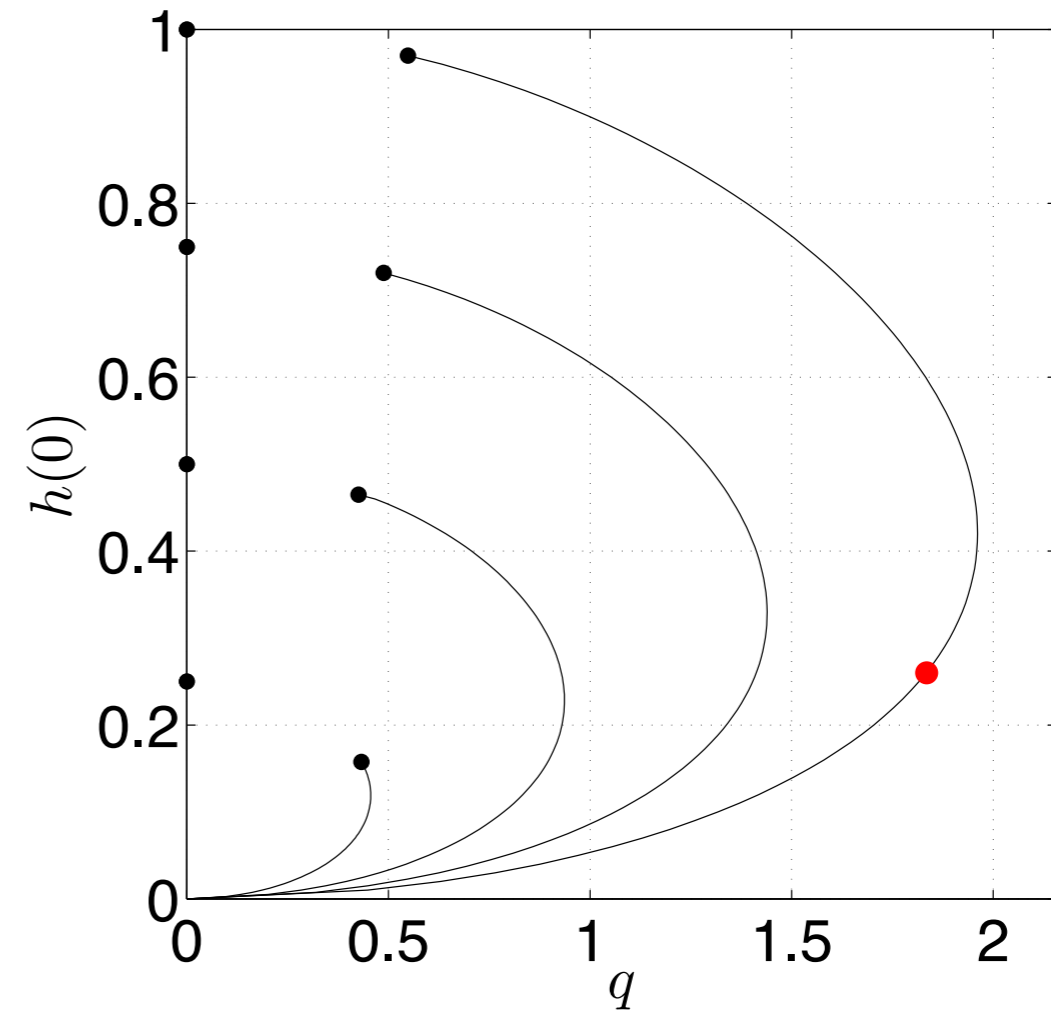
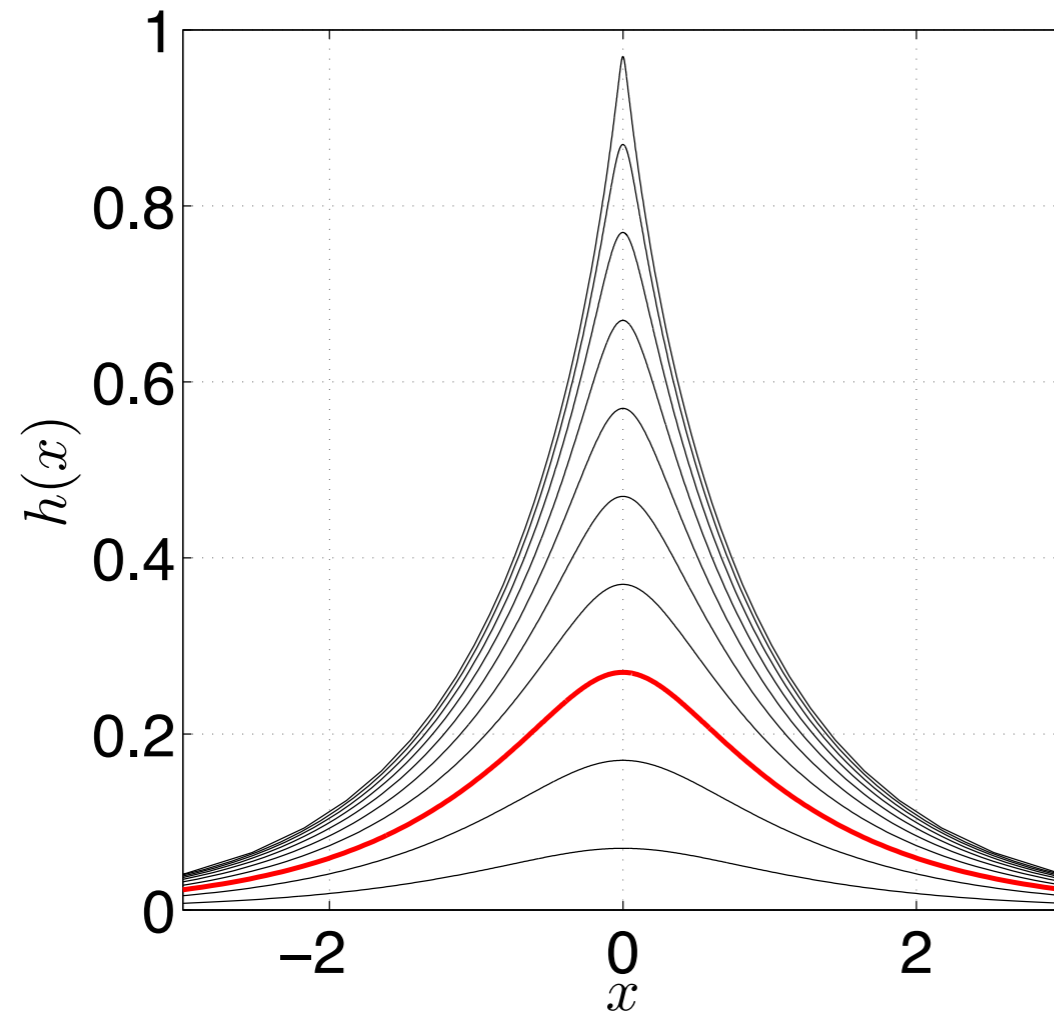
Computed Solutions



Left: computed solutions with $l = 1$, $M = 256$.

Right: q - $h(0)$ bifurcation diagrams for $l \in \{0.25, 0.5, 0.75, 1\}$.

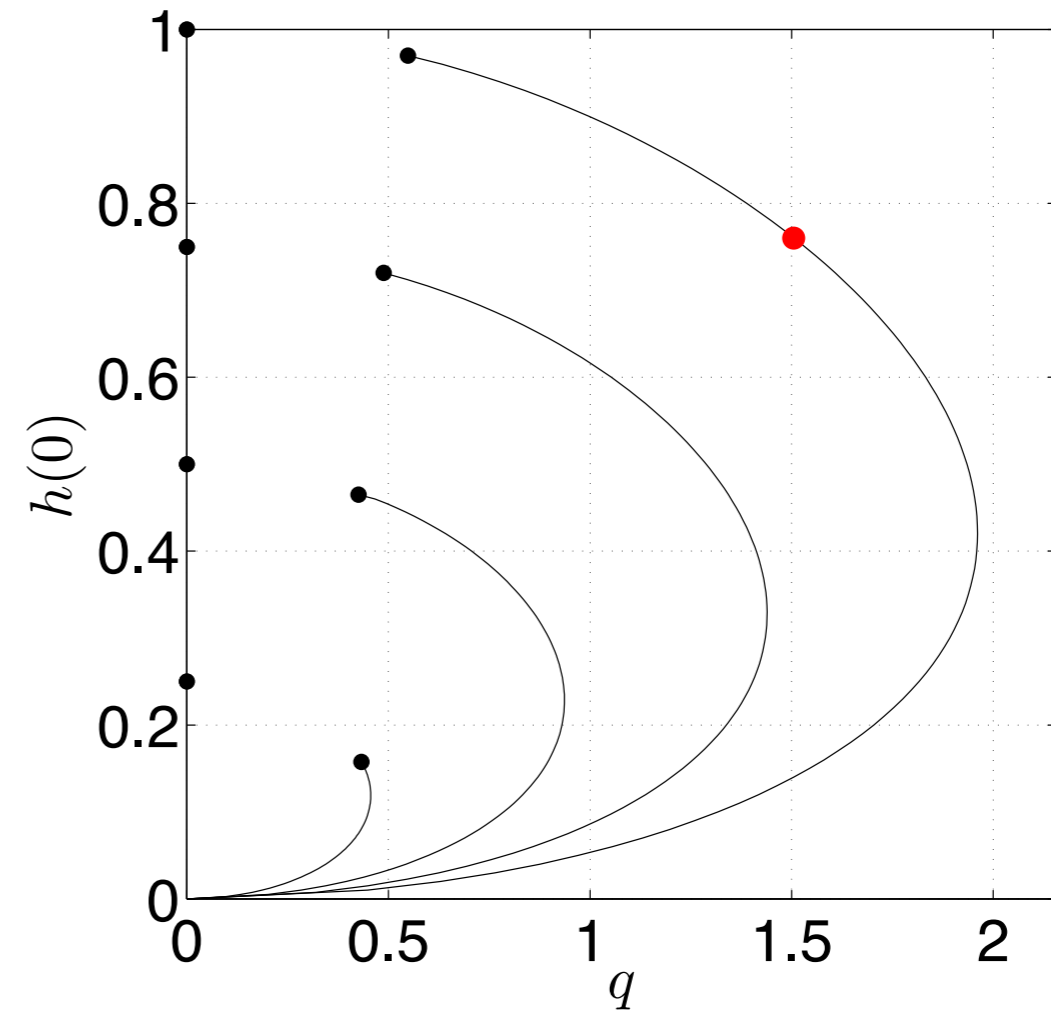
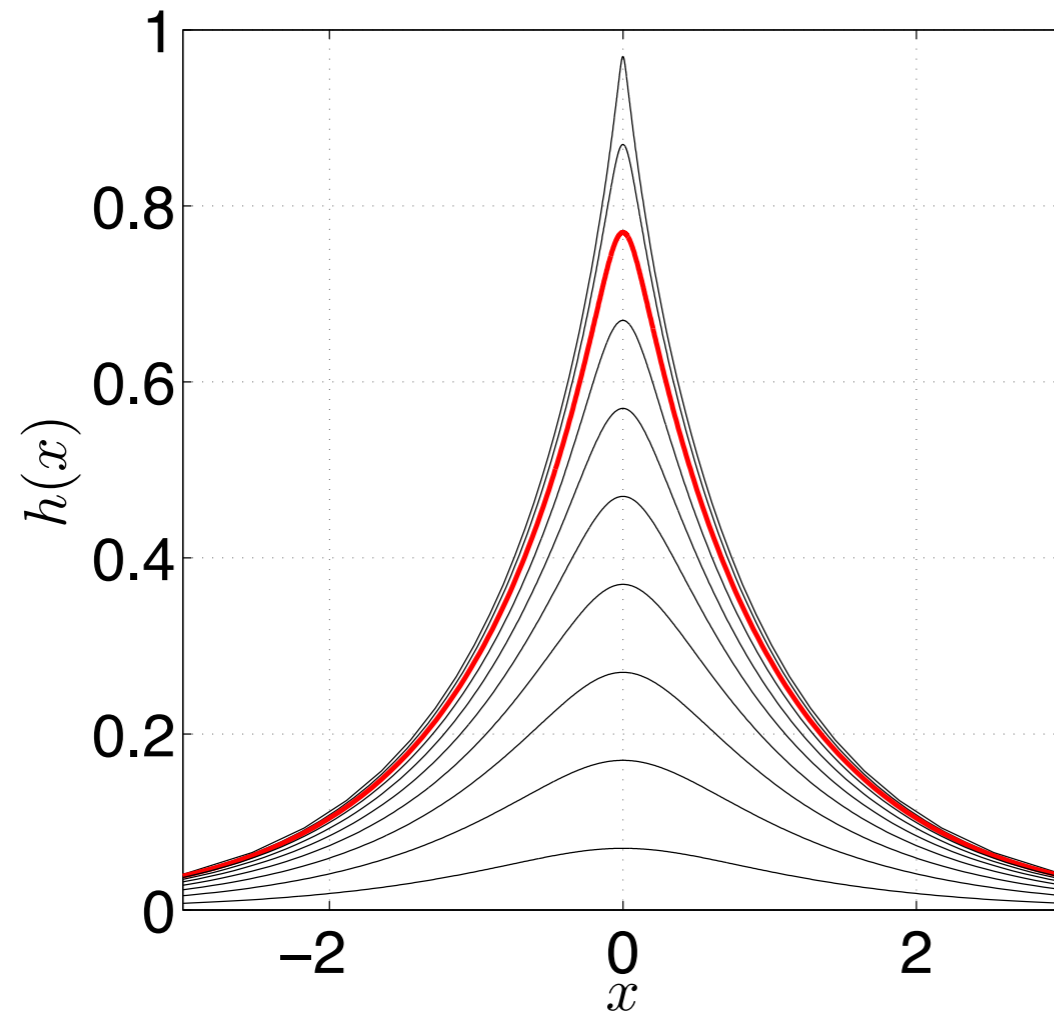
Computed Solutions



Left: computed solutions with $l = 1$, $M = 256$.

Right: q - $h(0)$ bifurcation diagrams for $l \in \{0.25, 0.5, 0.75, 1\}$.

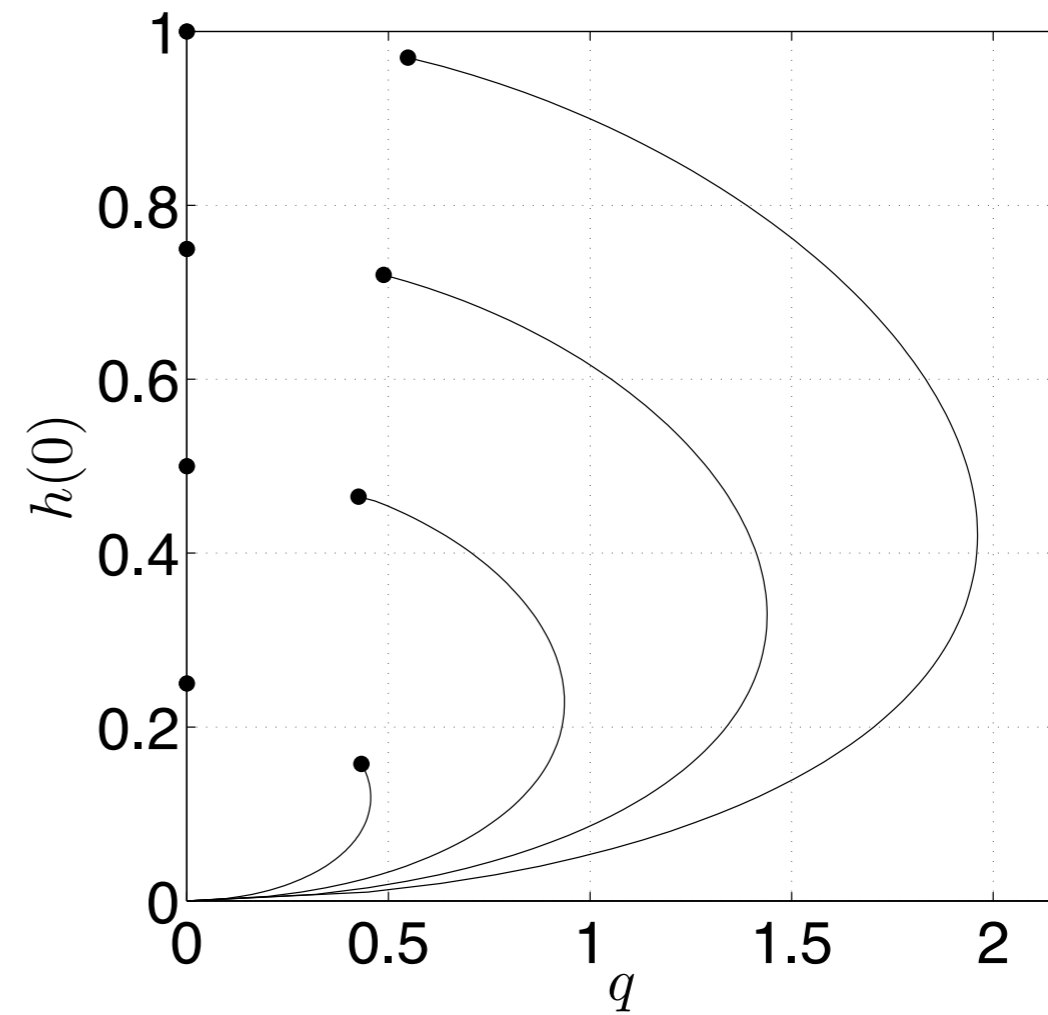
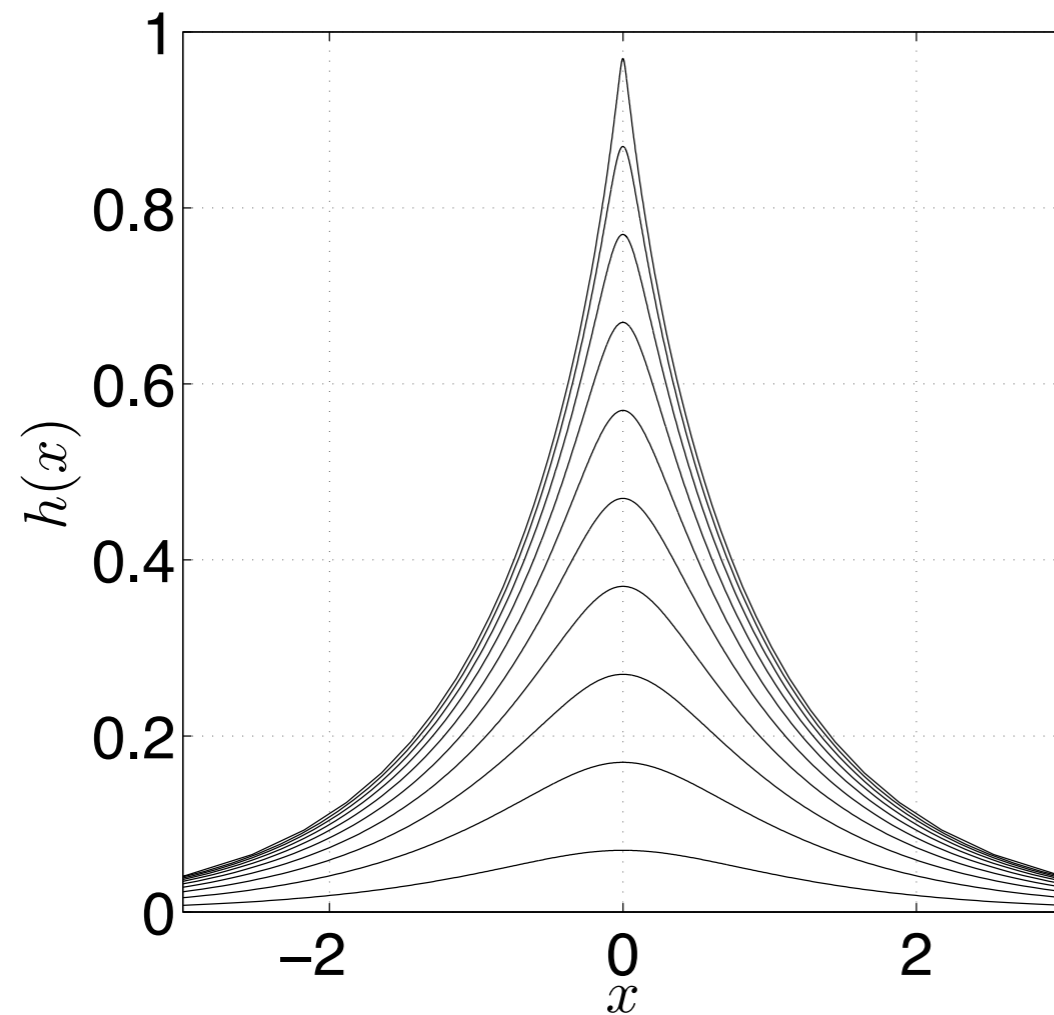
Computed Solutions



Left: computed solutions with $l = 1$, $M = 256$.

Right: q - $h(0)$ bifurcation diagrams for $l \in \{0.25, 0.5, 0.75, 1\}$.

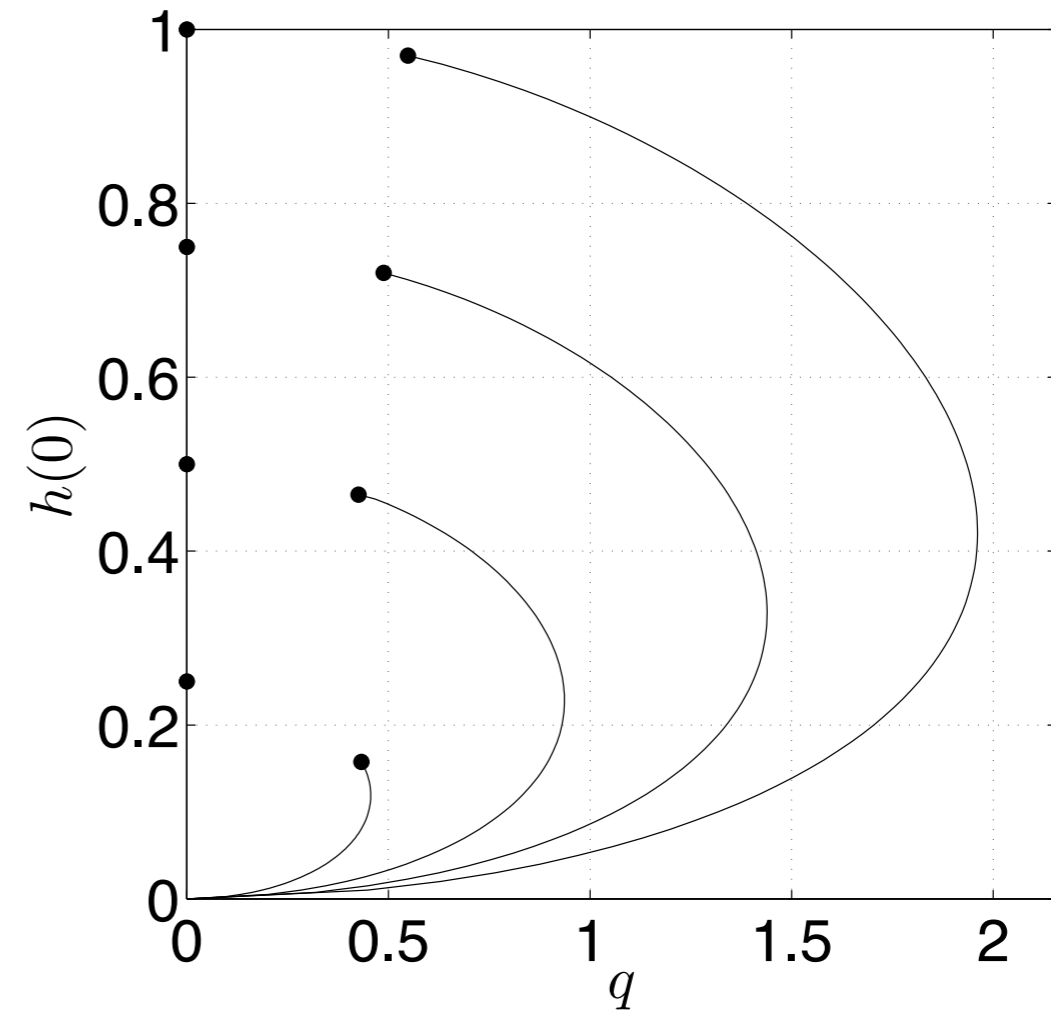
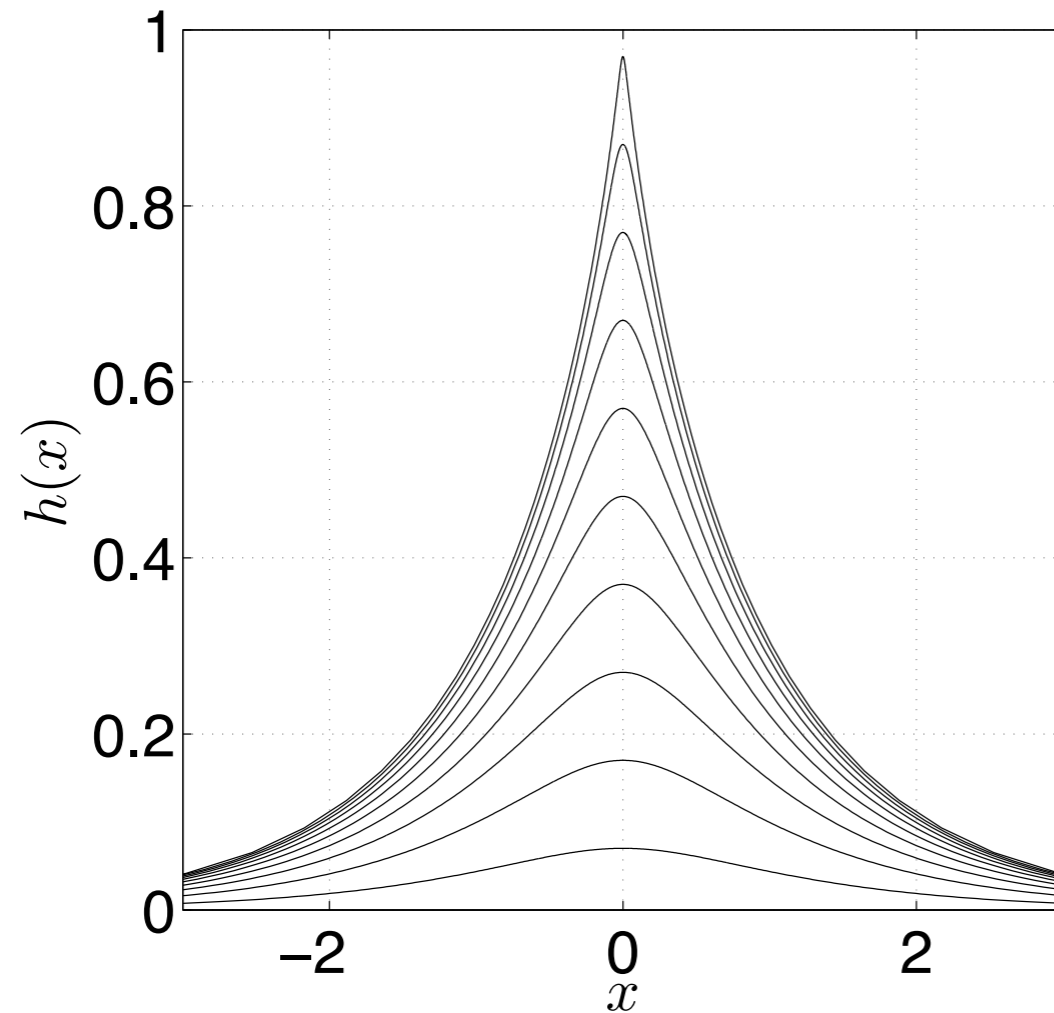
Computed Solutions



Saddle-node bifurcation corresponds to *pull-in*.

Define $\varepsilon = l - h(0)$.

Computed Solutions

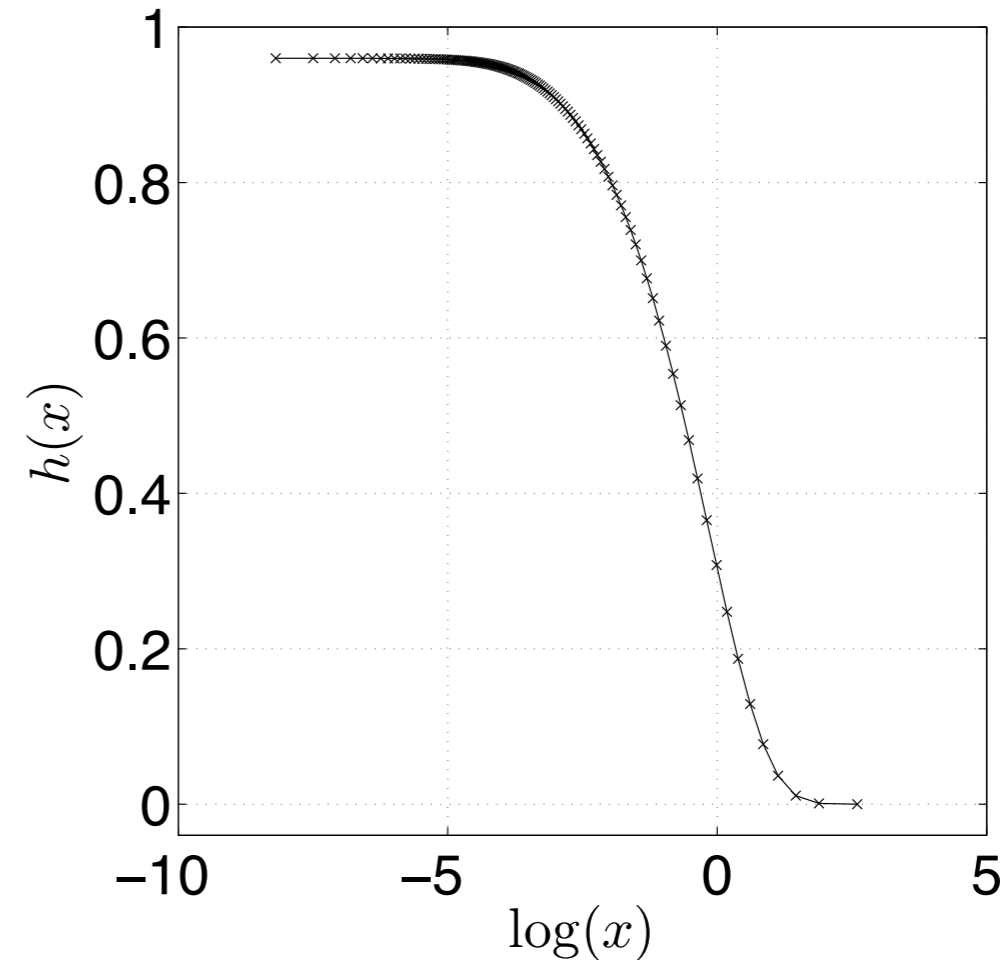
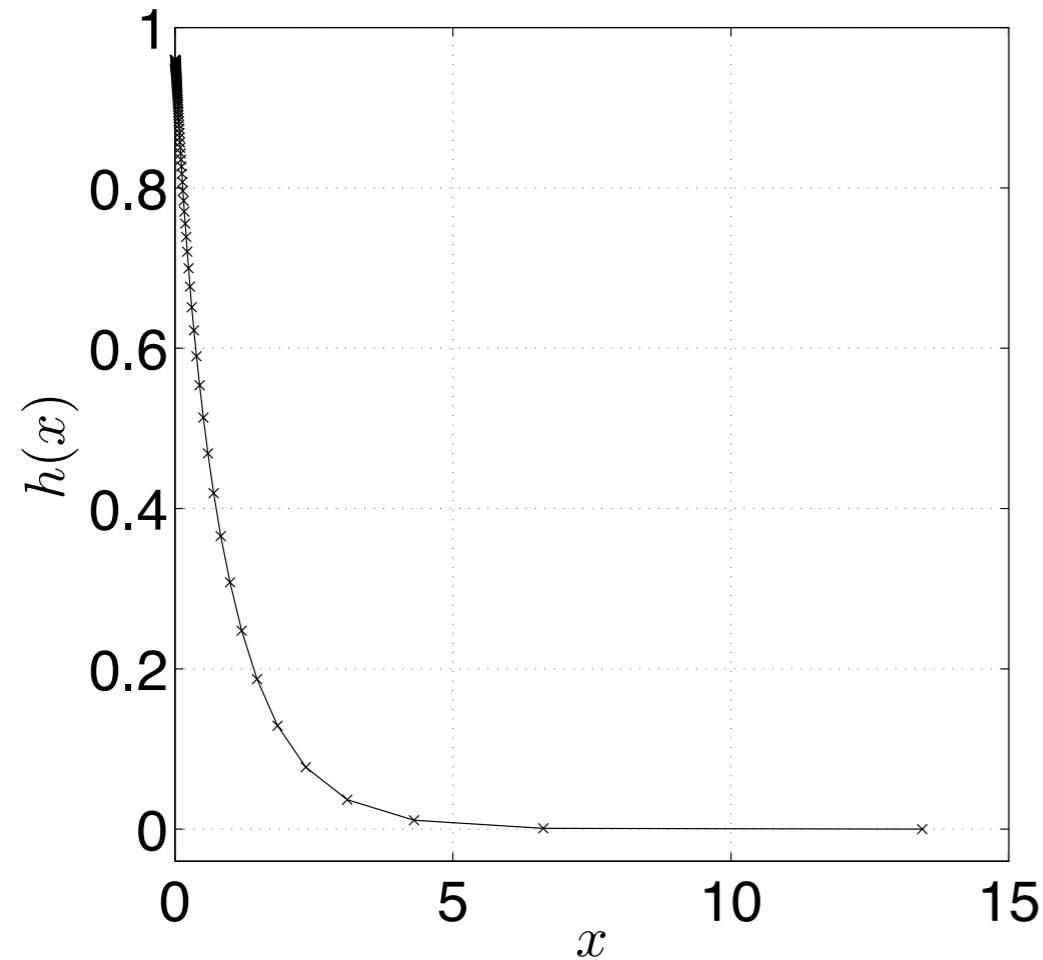


Interface tips sharpen and approach a corner as $\varepsilon \rightarrow 0$.

Collocation method fails for small ε in each case.

Computed Solution Resolution

$$l = 1, h(0) = 0.96 \ (\varepsilon = 0.04), M = 256:$$



Left: Small- ε profiles are poorly resolved for large x .

Right: Small- ε profiles are well-resolved for small x .

Crowding

Under a conformal map, equally spaced nodes on the unit circle concentrate near re-entrant corners and spread away from “convex” corners.

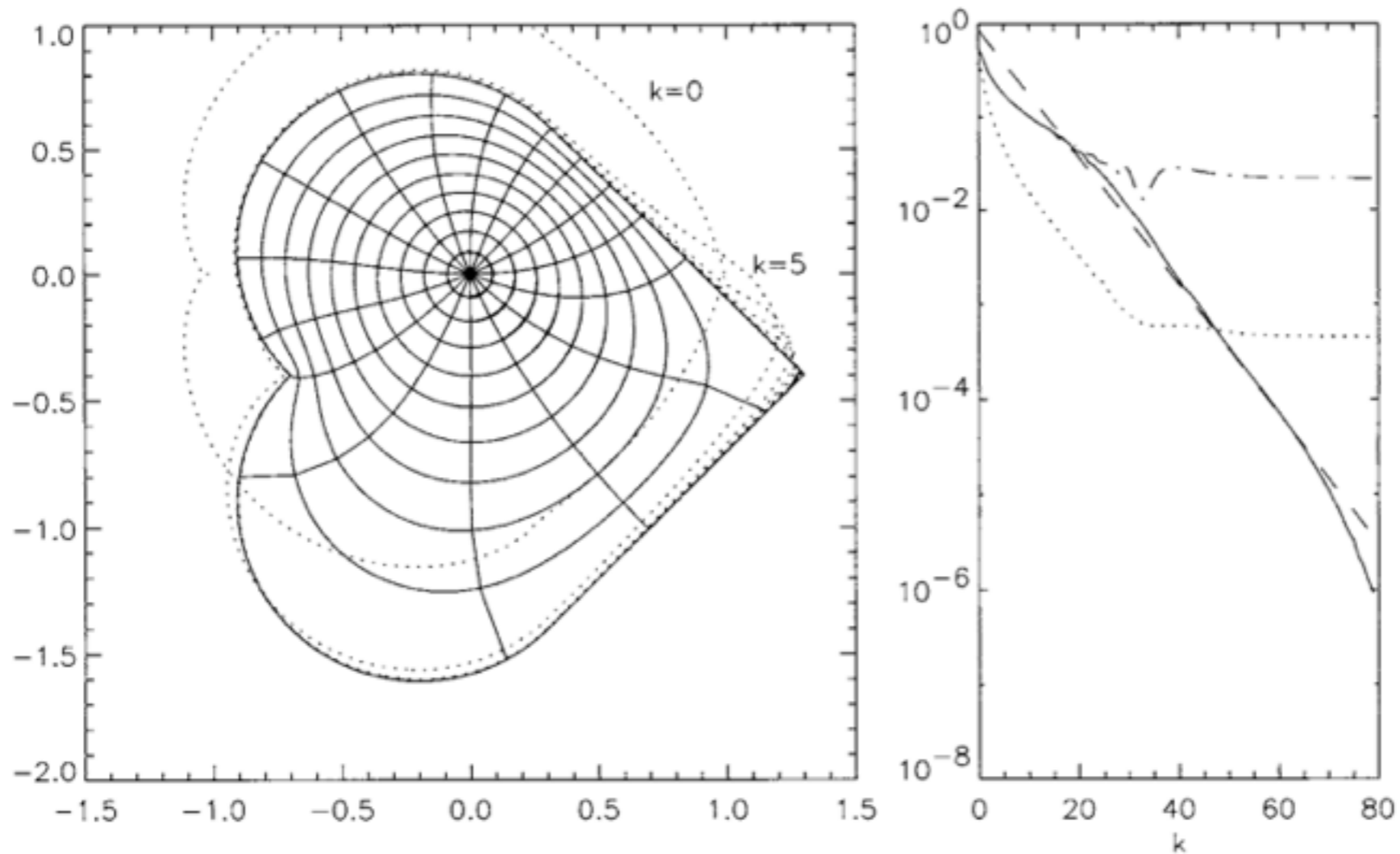
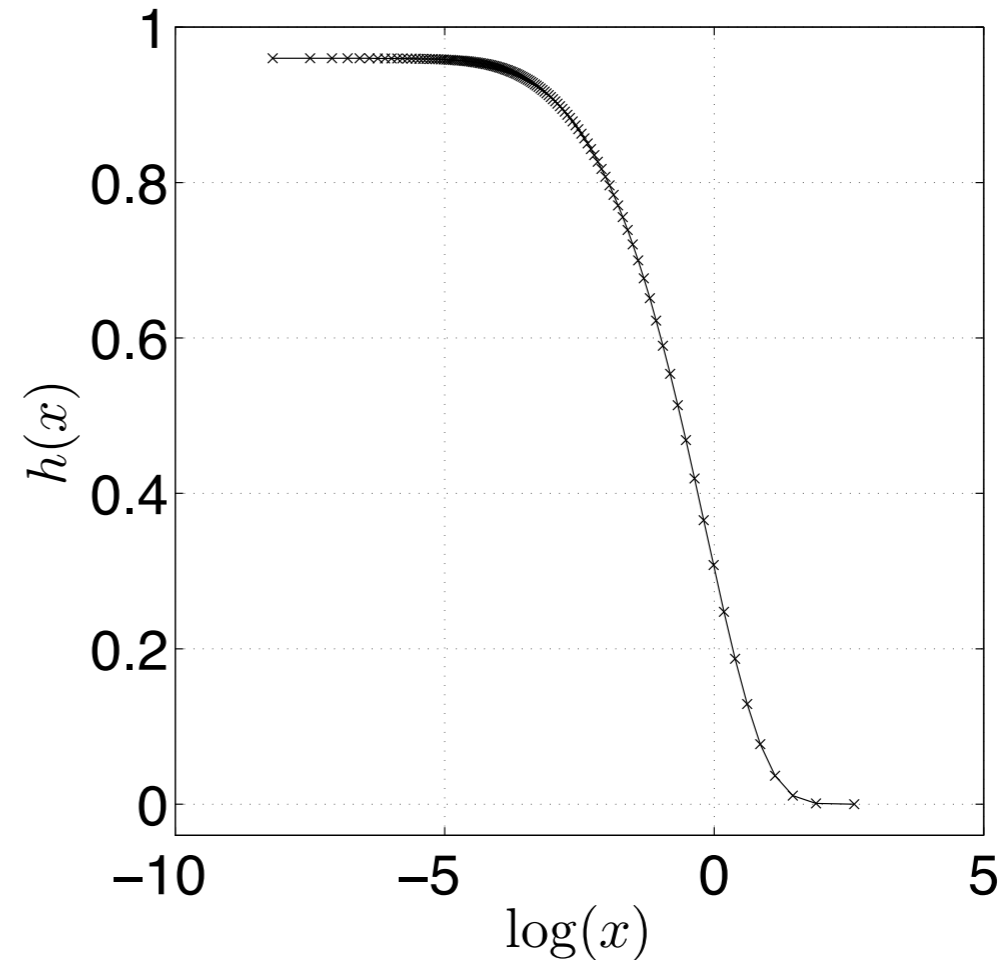
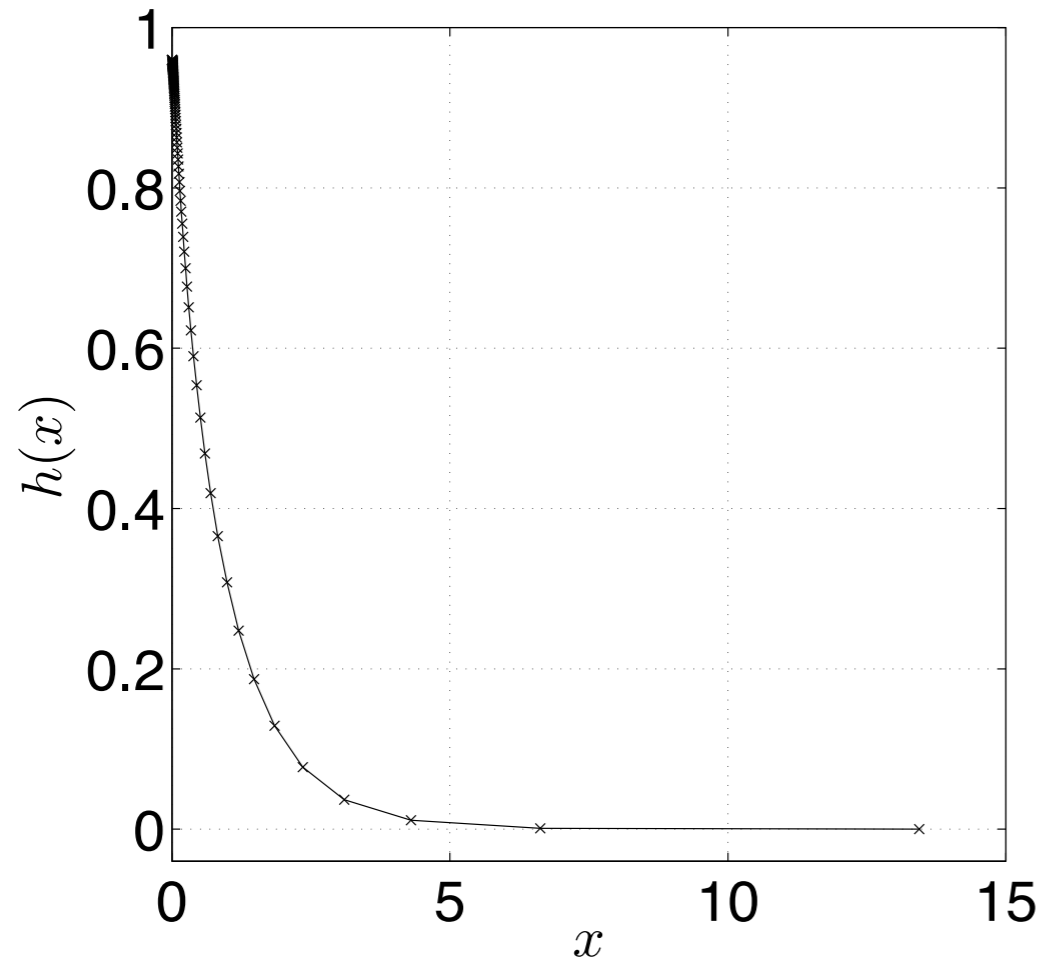


Fig. 8. The same as Figure 7 for the conformal mapping from the unit disk to the heart of Example 3 calculated by the smoothed AP method.

Computed Solution Resolution

$$l = 1, h(0) = 0.96 \ (\varepsilon = 0.04), M = 256:$$

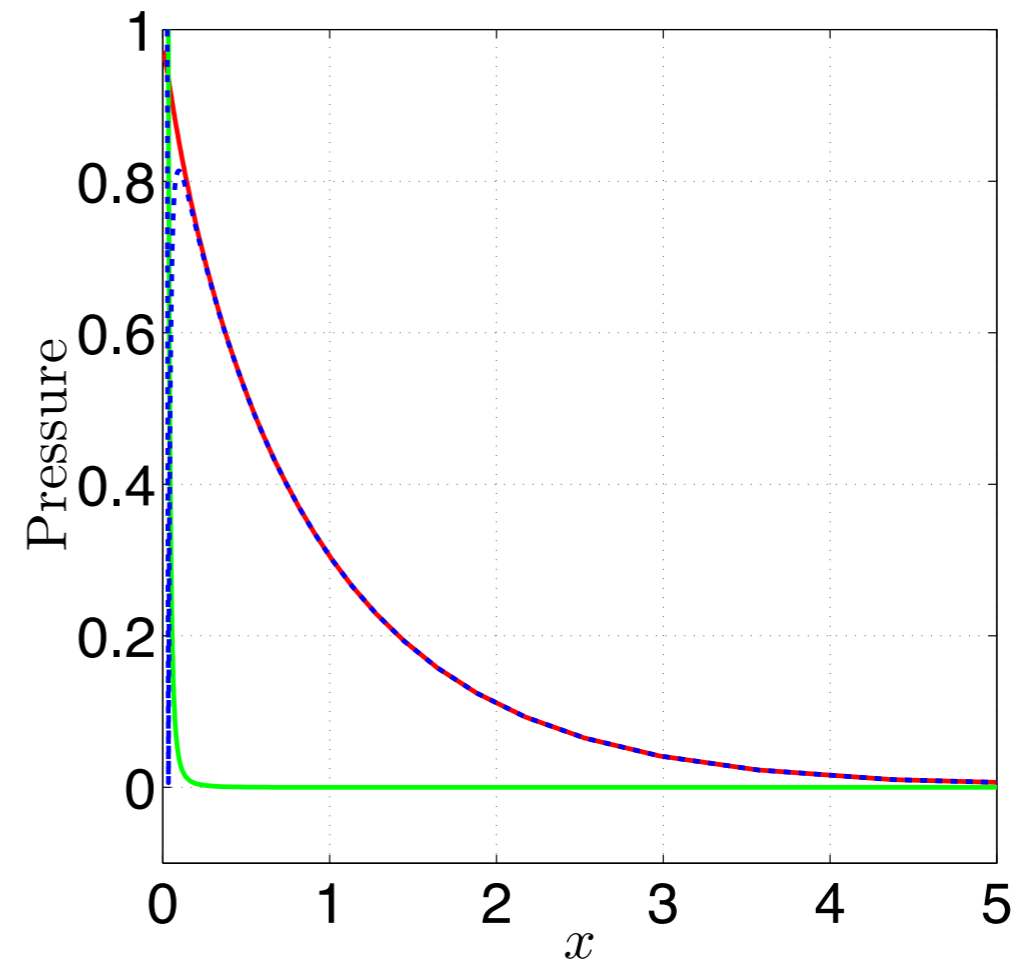
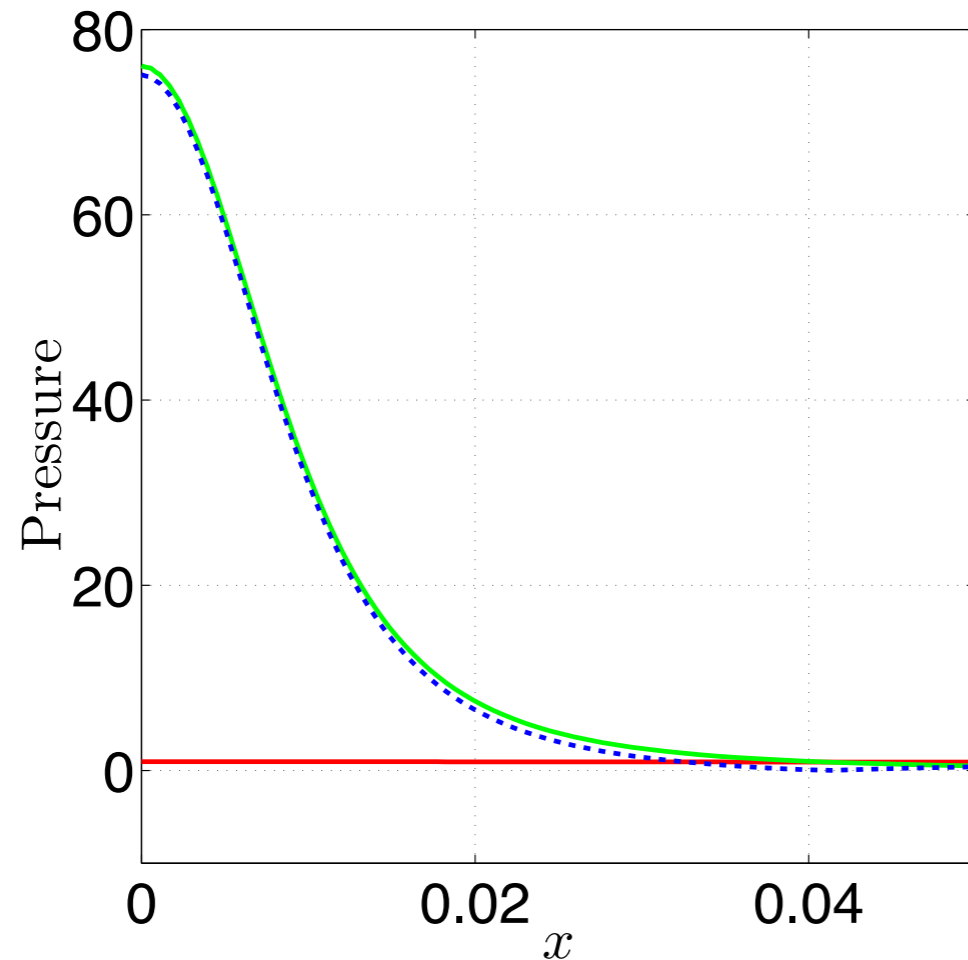


Left: Small- ε profiles are poorly resolved for large x .

Right: Small- ε profiles are well-resolved for small x .

Pressure Balances

$$l = 1, h(0) = 0.96, \varepsilon = 0.04:$$

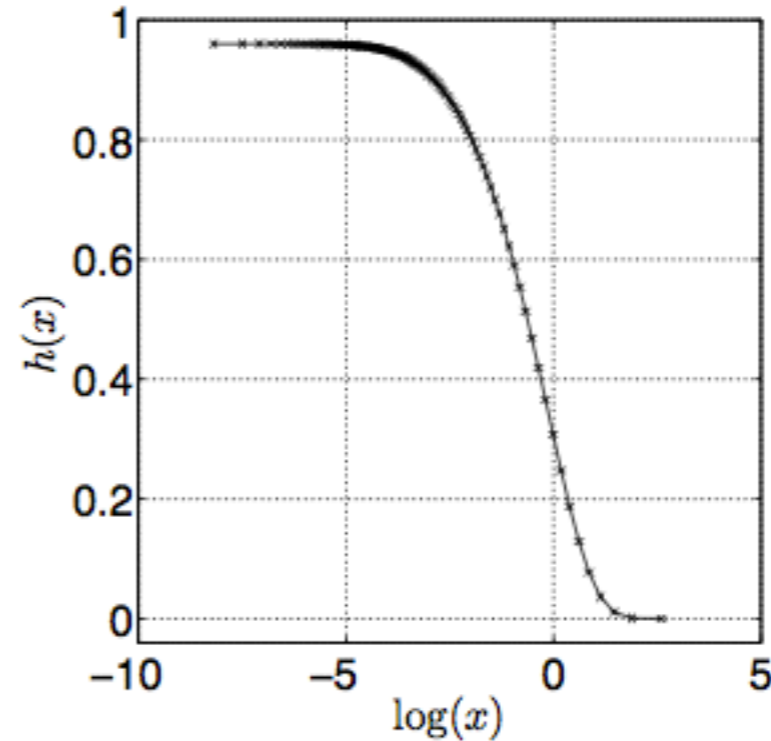
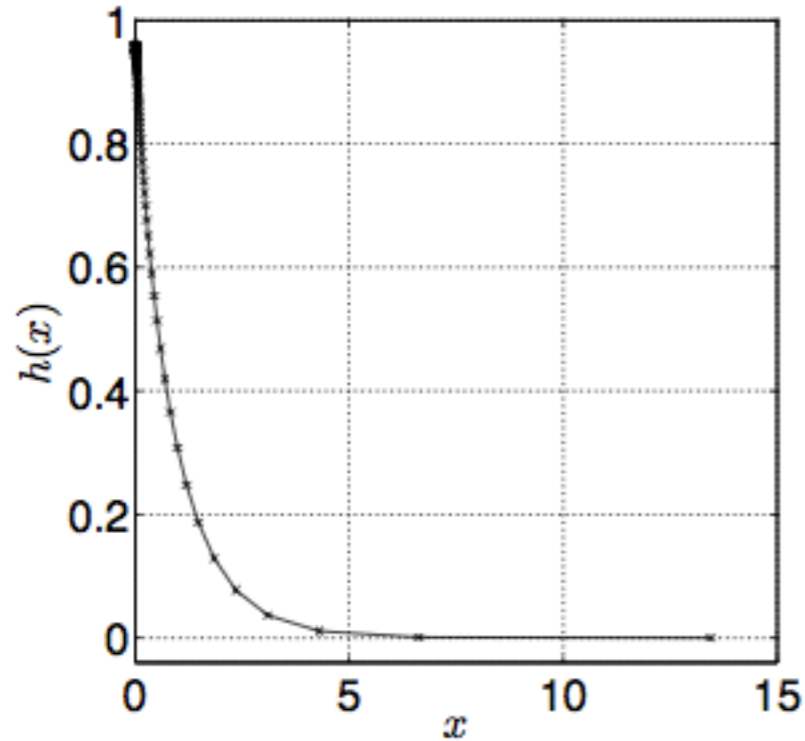


Separation motivates consideration of ‘inner’ and ‘outer’ regions independently.

The main challenge is then recombination.

Scaling for the “sharp” corners

$l = 1, h(0) = 0.96$ ($\epsilon = 0.04$), $M = 256$:



Charge concentrates at the tip:

$$F = \frac{q^2}{2\pi\epsilon} \delta(x)$$

$$h - \frac{h''}{(1 + h'^2)^{3/2}} = F$$

Concentrated charge approximation

Away from the interface tip, leading order profile h_0 satisfies:

$$\underbrace{\frac{h_{0,xx}(x)}{(1 + h_{0,x}^2(x))^{3/2}}}_{\text{elastic}} - \underbrace{h_0(x)}_{\text{gravitational}} = 0.$$

Solutions exist for $h_0(0) < \sqrt{2}$ and feature a corner at the tip:

$$h_{0,x}(0^\pm) = \mp \frac{h_0(0) \sqrt{4 - h_0^2(0)}}{2 - h_0^2(0)}.$$

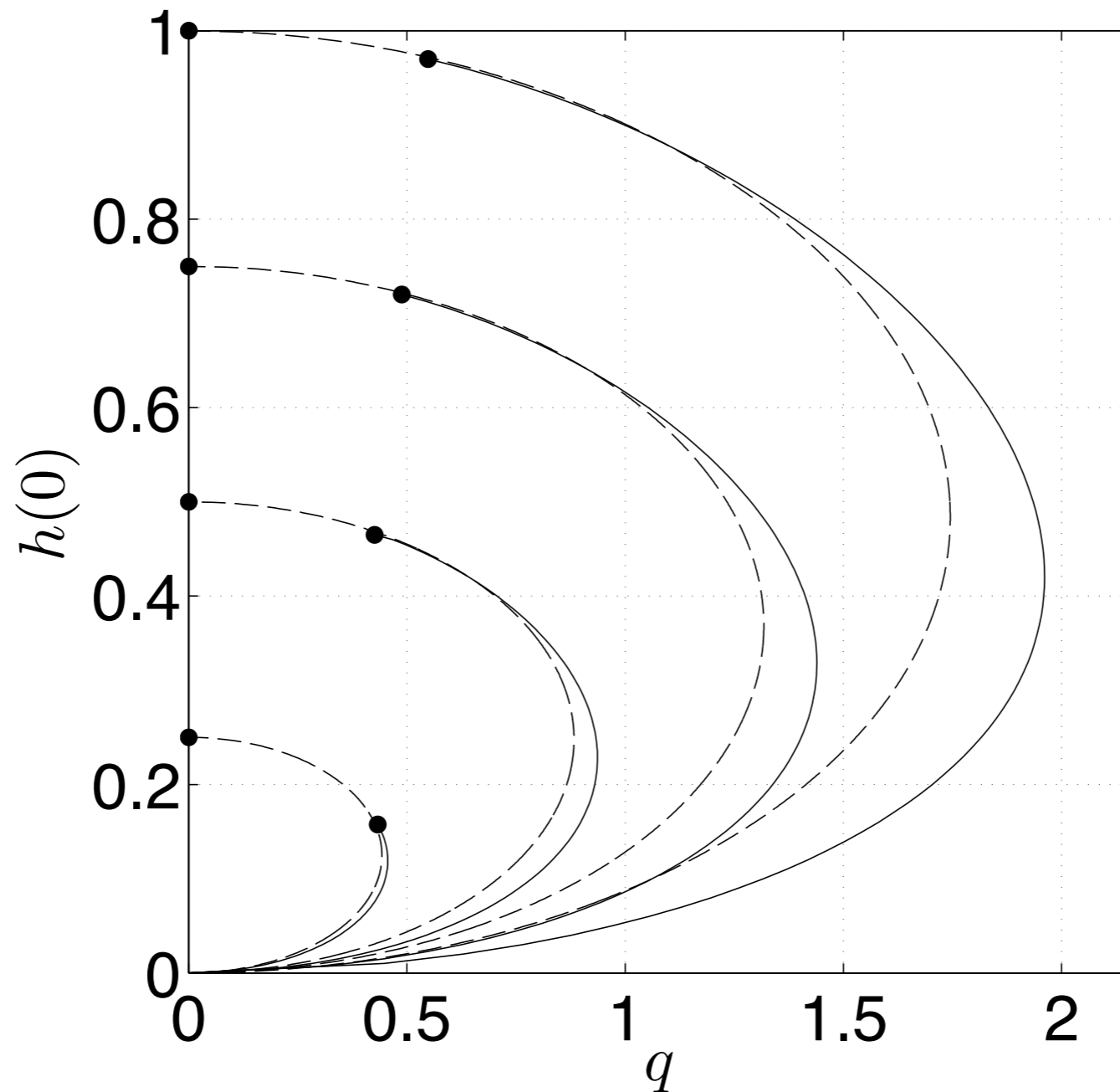
Denote the outer tip angle by $\pi/\gamma(h_0(0))$.

An implicit closed form representation can be computed.

$$2\gamma(h_0(0)) = F \approx \frac{q^2}{2\pi\epsilon} \approx \frac{q^2}{2\pi(l - h_0(0))}$$

Leading order bifurcation diagram

$$q = \sqrt{\left(2\pi h_0 \sqrt{4 - h_0^2}\right) (l - h_0) + O(\epsilon^{3/2})}$$



Outer Solution Symmetry

Governing equation may be recast:

$$\underbrace{\frac{\operatorname{Im}(f_{\theta\theta}(e^{i\theta})\overline{f_{\theta}(e^{i\theta})})}{|f_{\theta}(e^{i\theta})|^3}}_{\text{elastic}} - \underbrace{\operatorname{Re}(f(e^{i\theta}))}_{\text{gravitational}} = 0.$$

Both terms depend on interface *shape* only.

We therefore expect the parametrization of the outer map to be irrelevant (matches intuition).

Outer Solution Symmetry

Symmetry of Outer Solutions

If f solves

$$\frac{\operatorname{Im}(f_{\theta\theta}(e^{i\theta})\overline{f_{\theta}(e^{i\theta})})}{|f_{\theta}(e^{i\theta})|^3} - \operatorname{Re}(f(e^{i\theta})) = 0,$$

then so does

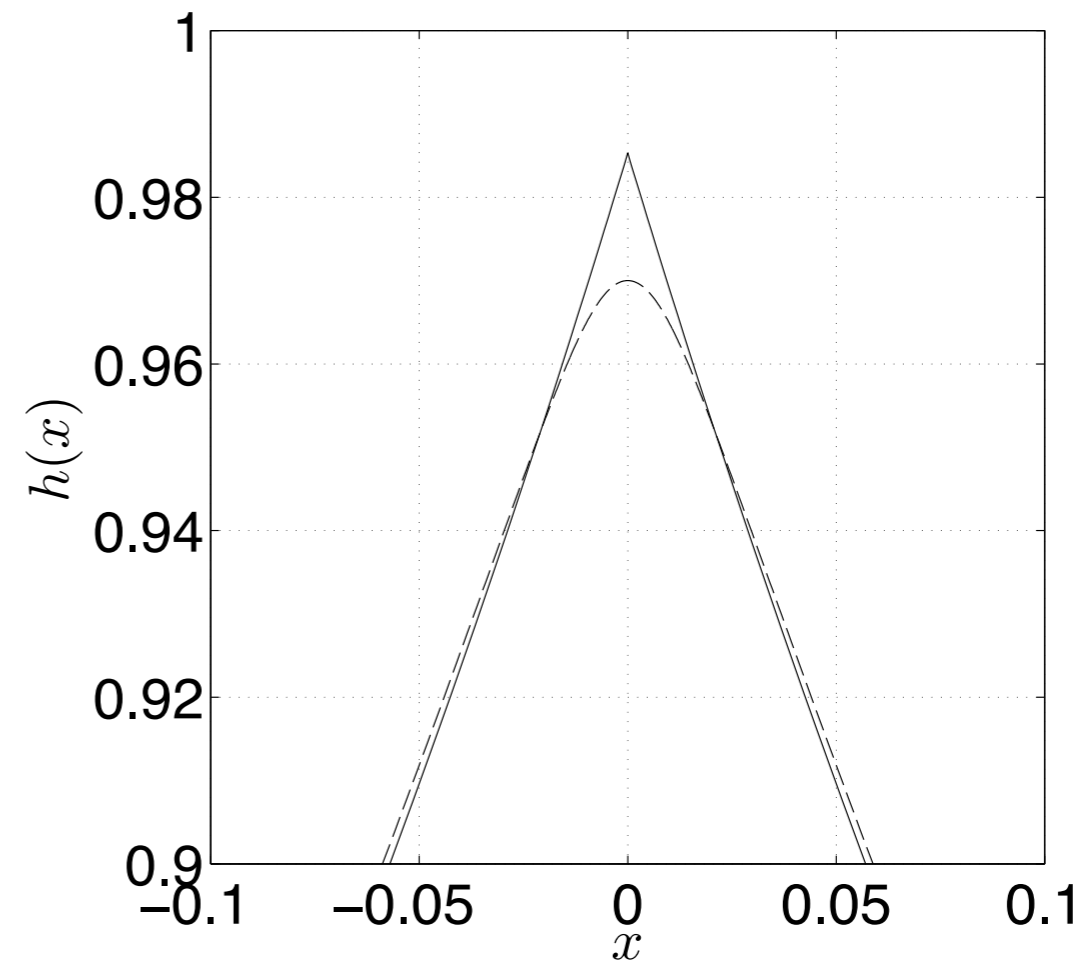
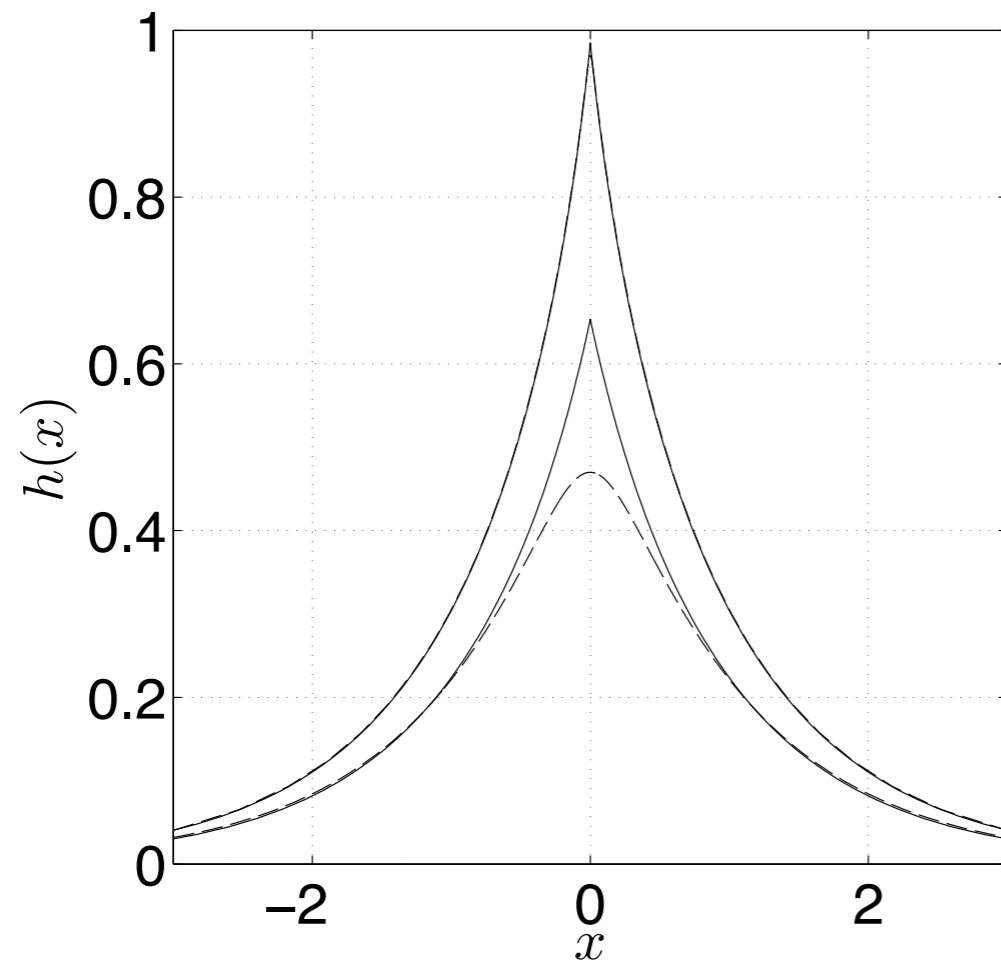
$$g(e^{i\theta}) = f(\mathcal{A}(e^{i\theta}))$$

where \mathcal{A} is any **conformal** automorphism (a bijective conformal map) from \mathbb{D} to itself.

$$\mathcal{A}_{\phi,b} = e^{i\phi} \frac{1 + bz}{\bar{b} + z} \quad \phi \in [0, 2\pi), |b| < 1$$

Computed Outer Solutions

Outer solutions (solid) vs full computed solutions (dashed),
 $l = 1, h_1(0) \in \{0.46, 0.96\}$:



Angled lines form boundary conditions for inner solutions.

Inner Solutions

Scaling $\mathbb{F} = \varepsilon F$, $q = \sqrt{\varepsilon}Q$:

$$\frac{\operatorname{Im}(F_{\theta\theta}(e^{i\theta})\overline{F_{\theta}(e^{i\theta})})}{|F_{\theta}(e^{i\theta})|^3} + \underbrace{\mathcal{O}(\varepsilon^2)}_{\text{gravity}} = -\frac{Q^2}{4\pi^2|F_{\theta}(e^{i\theta})|^2}.$$

All remaining terms depend on derivatives of \mathbb{F} only.

Inner Solutions

Scaling $\mathbb{F} = \varepsilon F$, $q = \sqrt{\varepsilon}Q$:

$$\frac{\operatorname{Im}(F_{\theta\theta}(e^{i\theta})\overline{F_{\theta}(e^{i\theta})})}{|F_{\theta}(e^{i\theta})|^3} + \underbrace{\mathcal{O}(\varepsilon^2)}_{\text{gravity}} = -\frac{Q^2}{4\pi^2|F_{\theta}(e^{i\theta})|^2}.$$

All remaining terms depend on derivatives of \mathbb{F} only.

Boundary conditions:

$$F(0) - F(1) = 1$$

(sets correct tip-charge separation)

Inner Solutions

Scaling $\mathbb{F} = \varepsilon F$, $q = \sqrt{\varepsilon}Q$:

$$\frac{\operatorname{Im}(F_{\theta\theta}(e^{i\theta})\overline{F_{\theta}(e^{i\theta})})}{|F_{\theta}(e^{i\theta})|^3} + \underbrace{\mathcal{O}(\varepsilon^2)}_{\text{gravity}} = -\frac{Q^2}{4\pi^2|F_{\theta}(e^{i\theta})|^2}.$$

All remaining terms depend on derivatives of \mathbb{F} only.

Boundary conditions:

$$F(0) - F(1) = 1$$

(sets correct tip-charge separation)

$$\arg(F(e^{i\theta})) \rightarrow e^{\pm i\pi/2\gamma} \text{ as } \theta \rightarrow \mp\pi$$

(matches inner limit of outer solutions)

Inner Solutions

Symmetry of Inner Solutions

If F solves

$$\frac{\operatorname{Im}(F_{\theta\theta}(e^{i\theta})\overline{F_{\theta}}(e^{i\theta}))}{|F_{\theta}(e^{i\theta})|^3} = -\frac{Q^2}{4\pi^2|F_{\theta}(e^{i\theta})|^2}$$

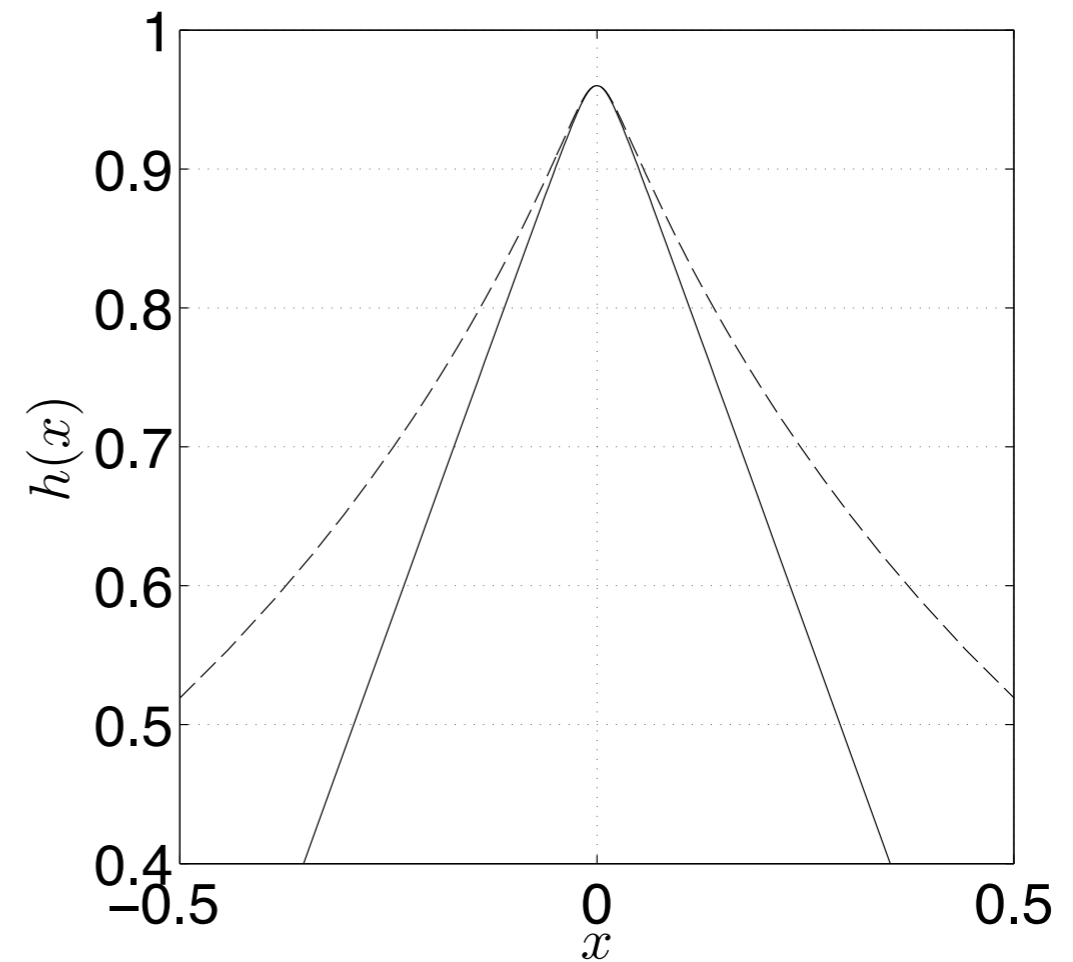
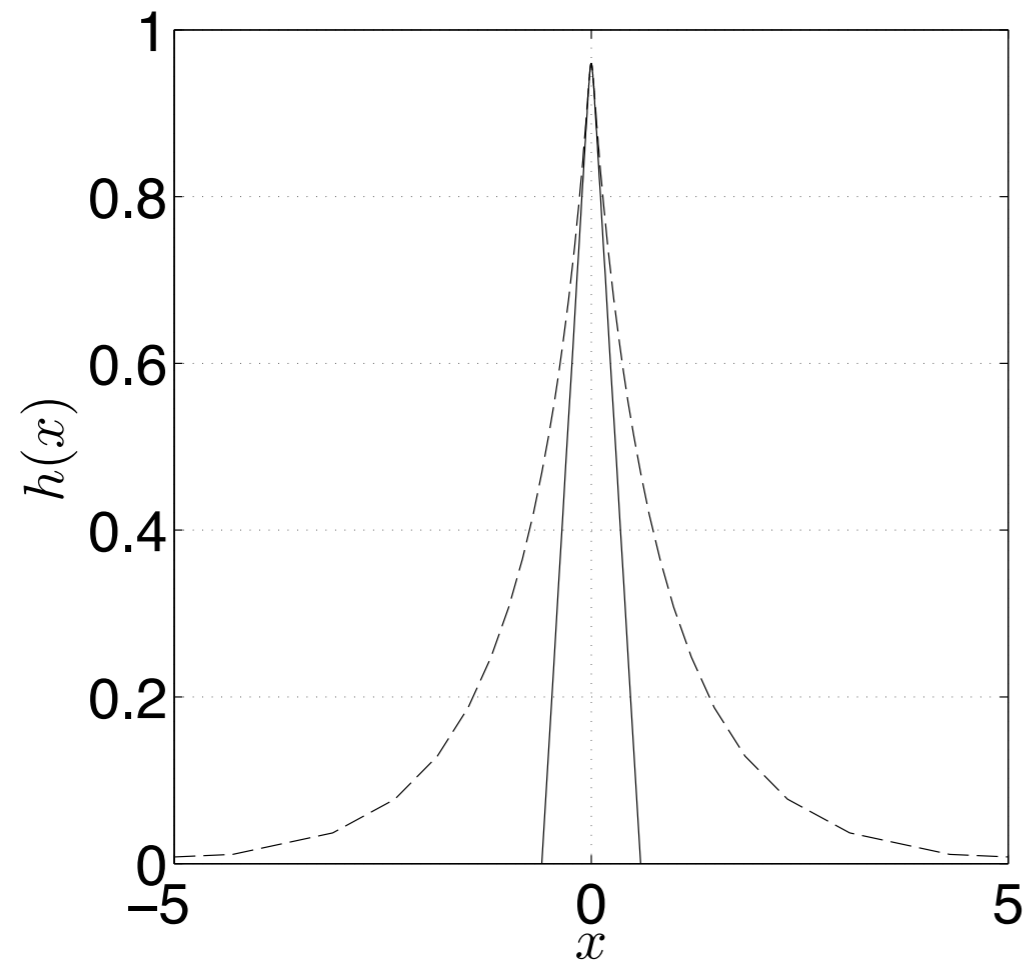
then so does

$$F + c$$

for any $c \in \mathbb{R}$.

Computed Inner Solutions

(Rescaled) inner solution (solid) vs full computed solution (dashed), $l = 1$, $h_1(0) = 0.96$:



Matched Solutions

Recall:

- Outer solutions can be conformally reparametrized.
- Inner solutions can be scaled and translated.

Posit solutions of the form:

$$\mathbb{G}(e^{i\theta}) = \left(\varepsilon G(e^{i\theta}) + H_0 \right) + g(\mathcal{A}(e^{i\theta})) - \mathcal{G}(e^{i\theta}).$$

1. G is an inner solution.
2. g is an outer solution.

Matched Solutions

Recall:

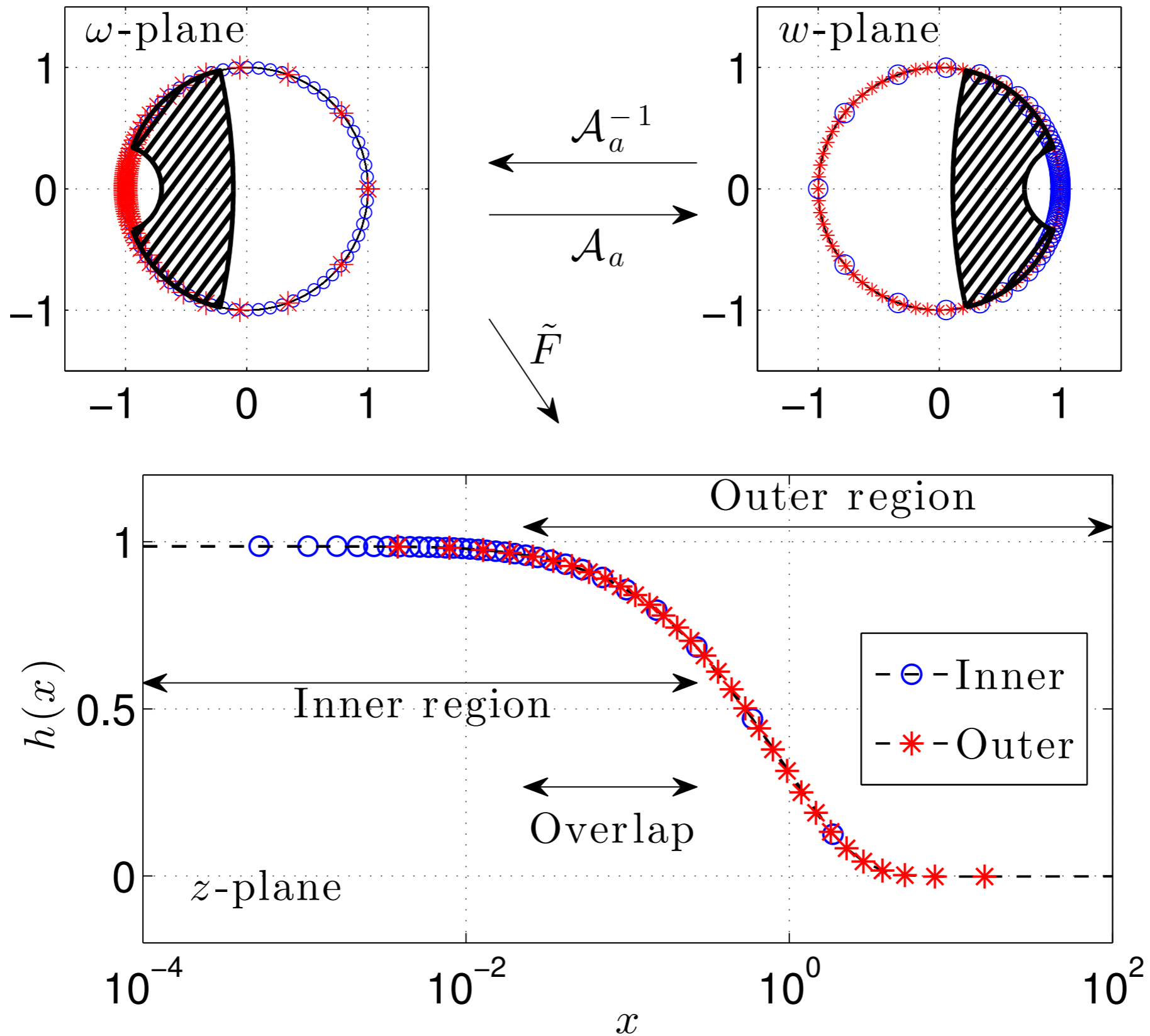
- Outer solutions can be conformally reparametrized.
- Inner solutions can be scaled and translated.

Posit solutions of the form:

$$\mathbb{G}(e^{i\theta}) = \left(\varepsilon G(e^{i\theta}) + H_0 \right) + g(\mathcal{A}(e^{i\theta})) - \mathcal{G}(e^{i\theta}).$$

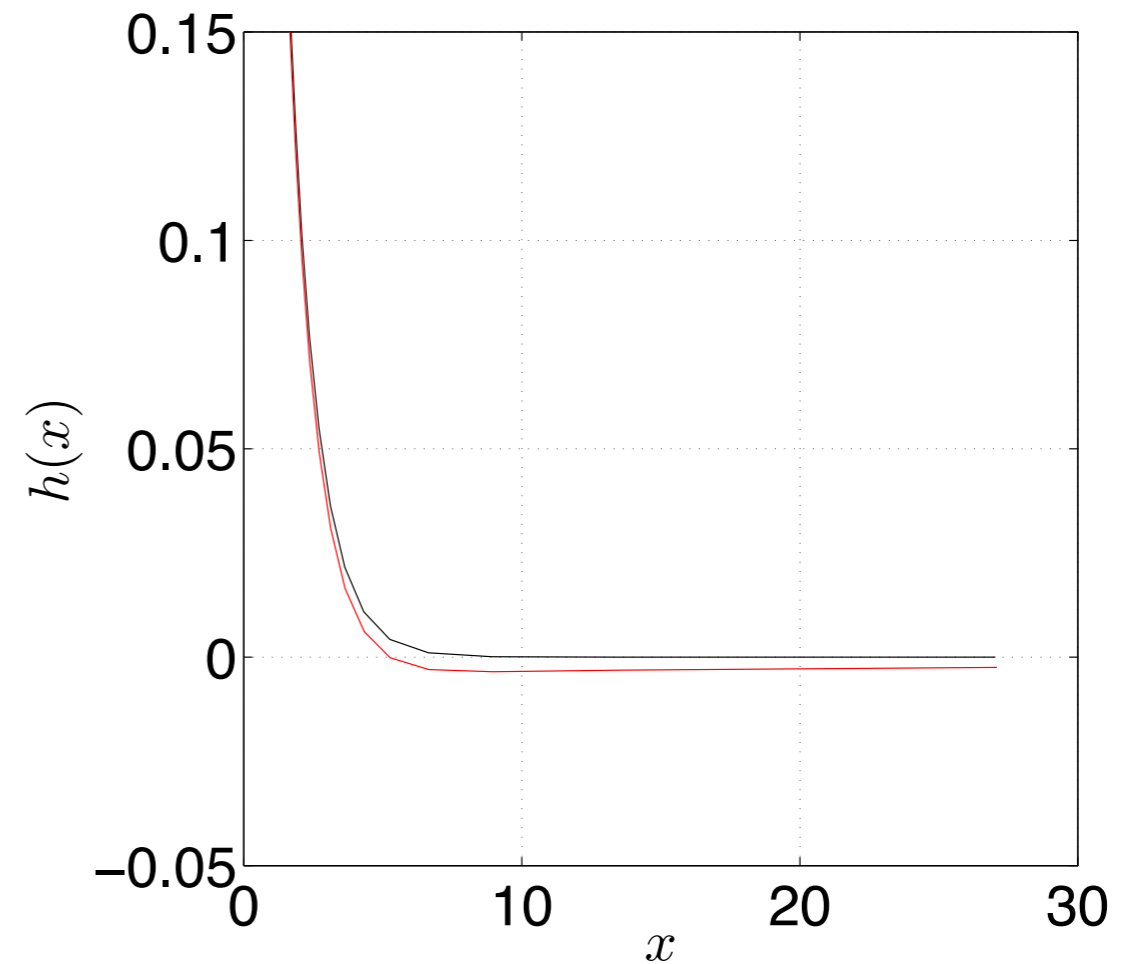
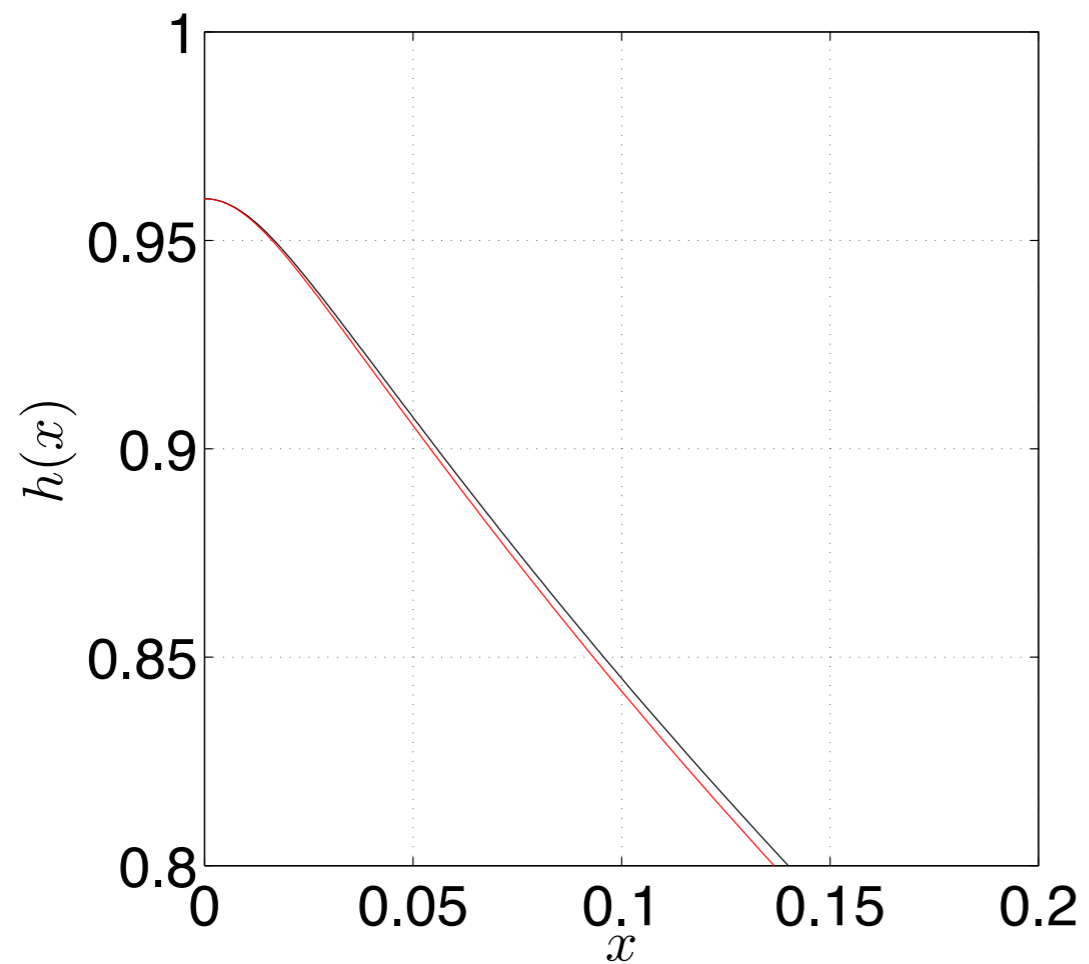
1. G is an inner solution.
2. g is an outer solution.
3. H_0 is a translation.
4. \mathcal{A} controls the parametrization of the outer solution.
5. \mathcal{G} is an ‘overlap function’.

What is matching?



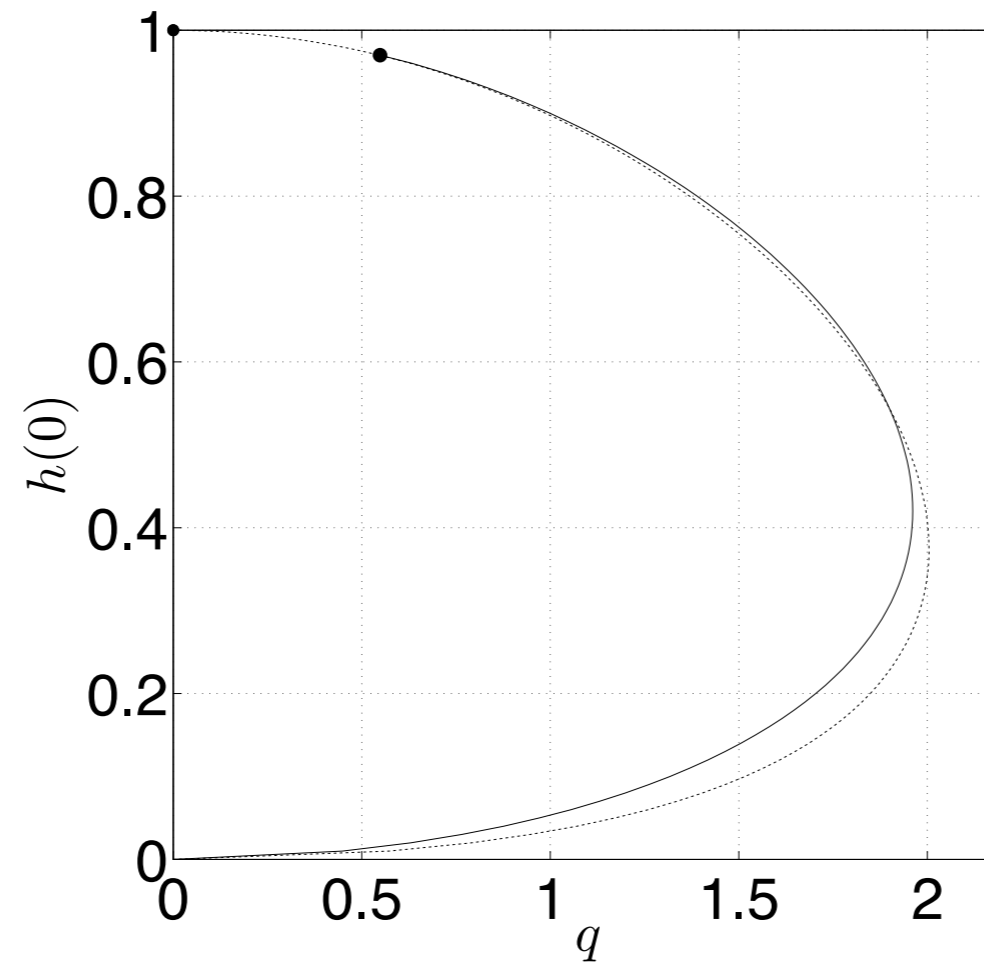
Matched Solutions

Matched solutions (red) vs full computed solutions (black),
 $l_1 = 1$, $h_1(0) = 0.96$ (equiv. $\varepsilon = 0.04$):



Matched Solutions

Example $q-h_1(0)$ bifurcation diagram:



Solid: full computed solutions

Dotted: matched solutions

Related work, open questions,...

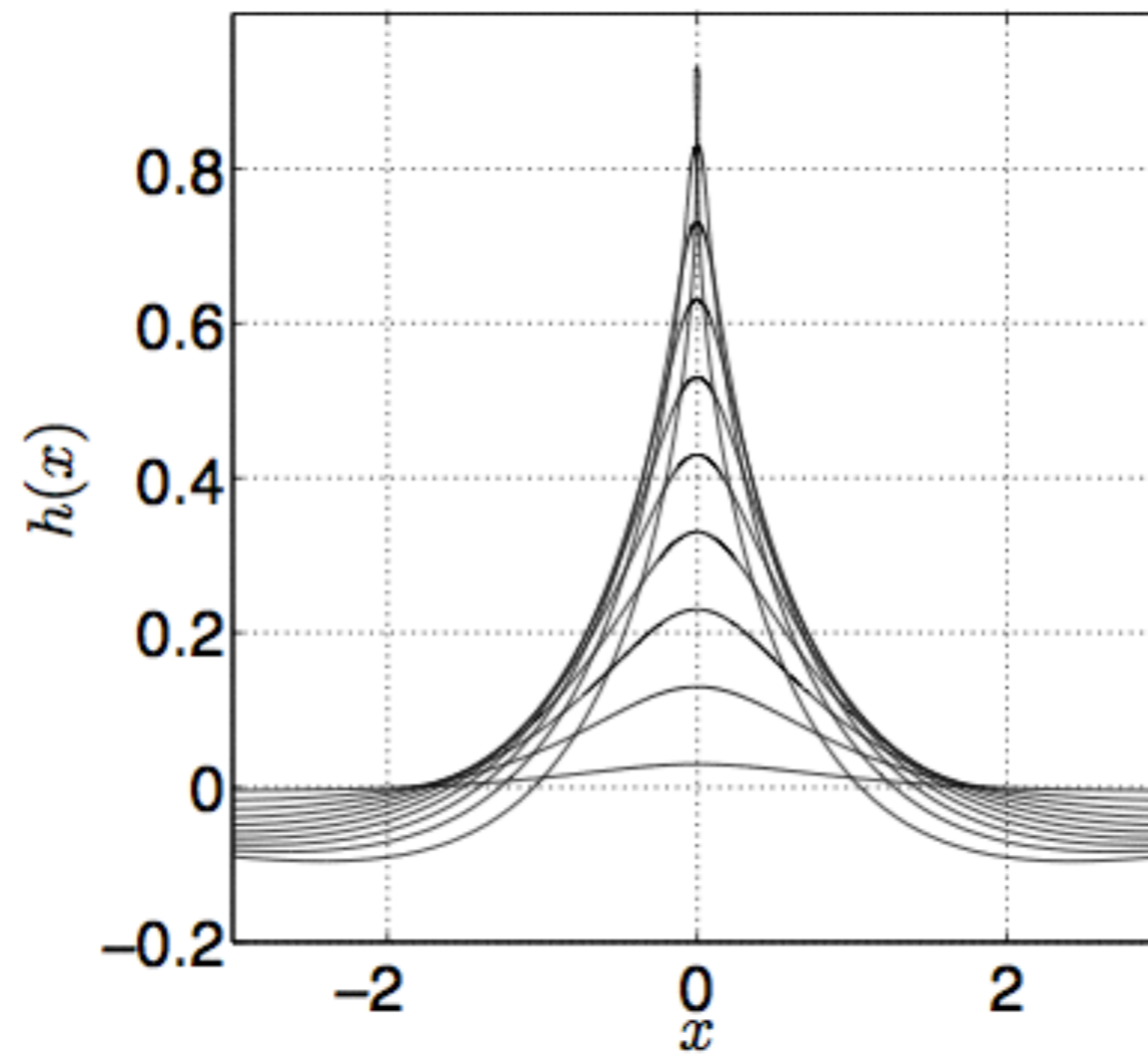
- Inverse problem and control: Design forcing for desired interface shape.
- Capillary effects: Undulations, droplet formation.
- Water waves: Wilkening (2011); Dyachenko, Lushnikov, and Korotkevich (2015).
- Conformal mappings in “Hybrid variables”: Crowdy, Tanveer and DeLillo (2014).
- Applications to regularized Hele-Shaw, DLA.

Open questions and ongoing work

- Fuller study of the $p = 1$ modified system with different types of forcing, Universality?
- Investigation of the $p = 2$ electrostatic problem with $l > \sqrt{2}$.
- Study of the resolutions of more general tip singularities in outer solutions (logarithmic for the modified system described, cusps).
- Application of our technique to other problems featuring sharpening geometry represented by conformal maps (Hele-Shaw, DLA).
- The inverse problem and control: design a forcing for a given interface shape.

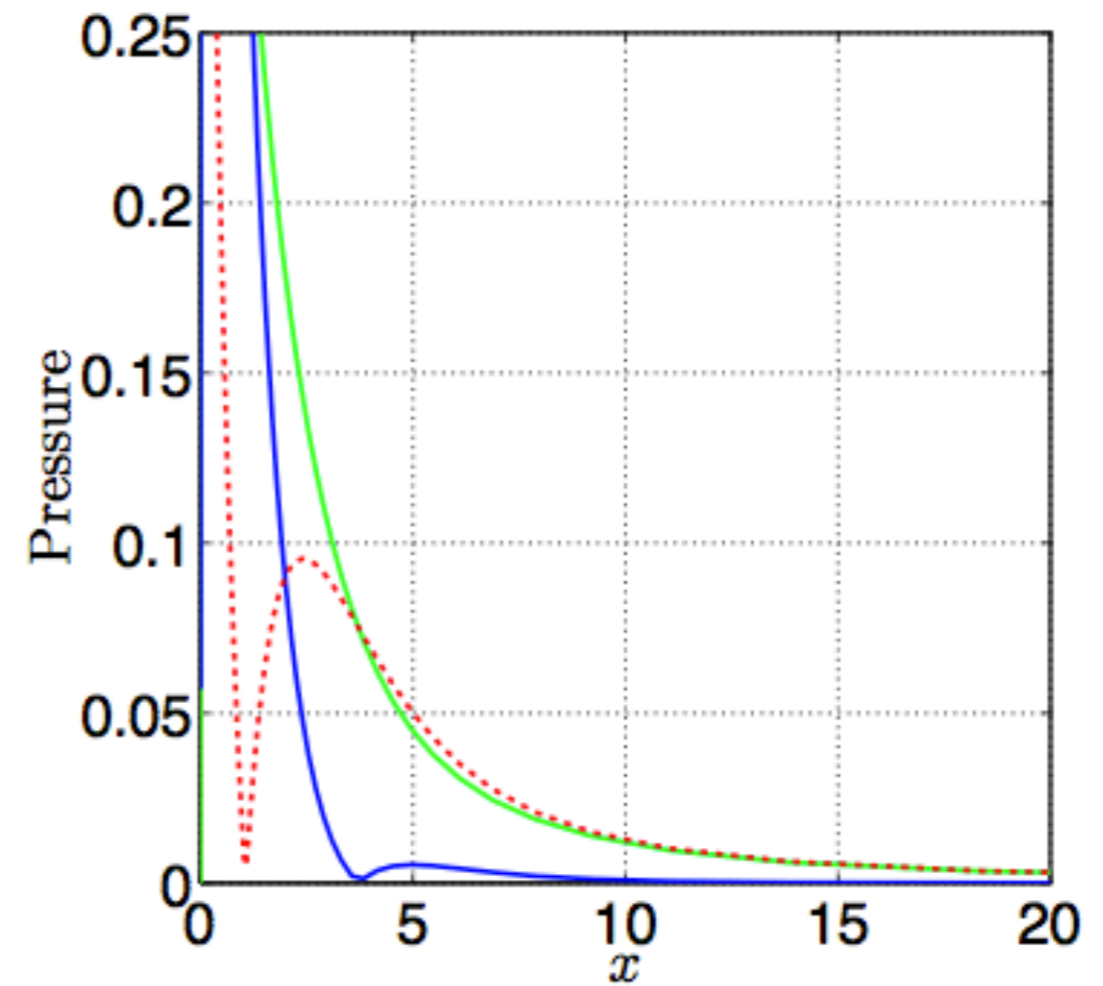
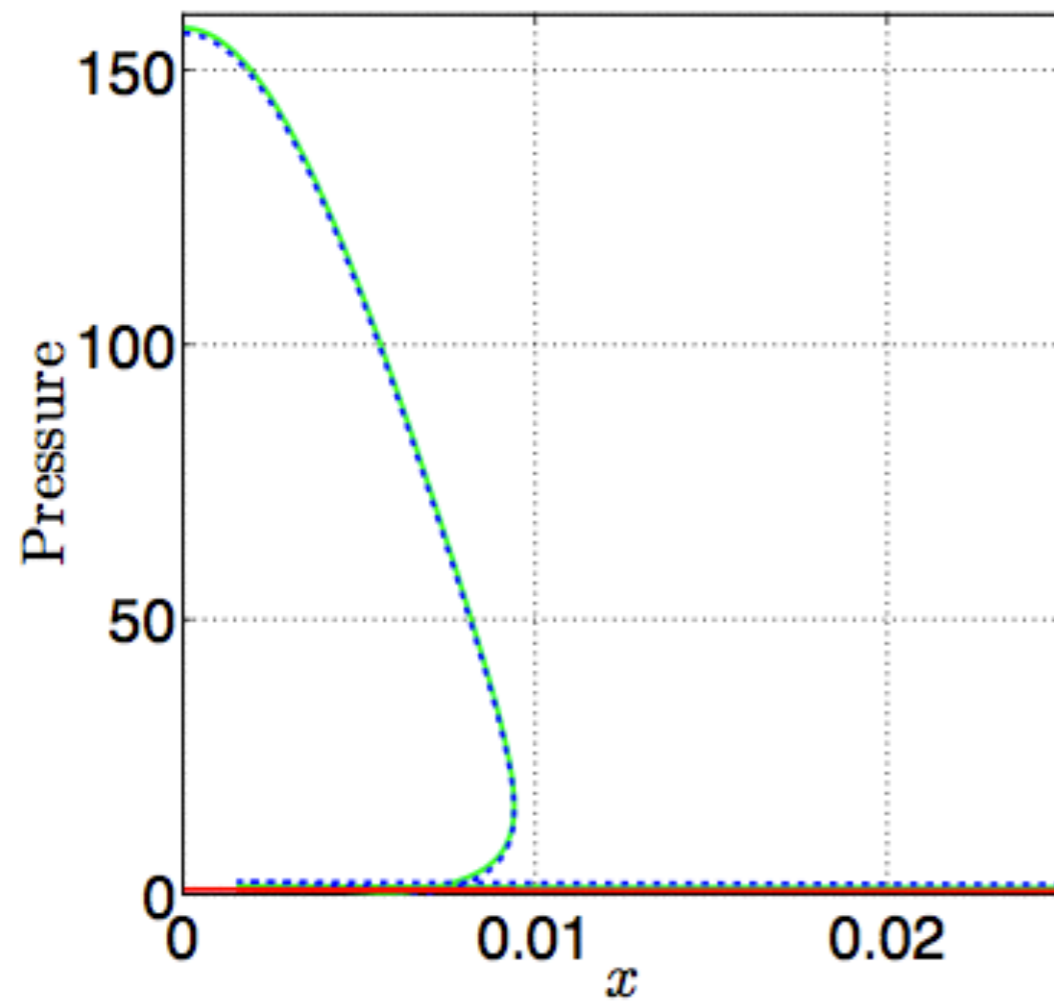
$\rho=1$, dipole forcing

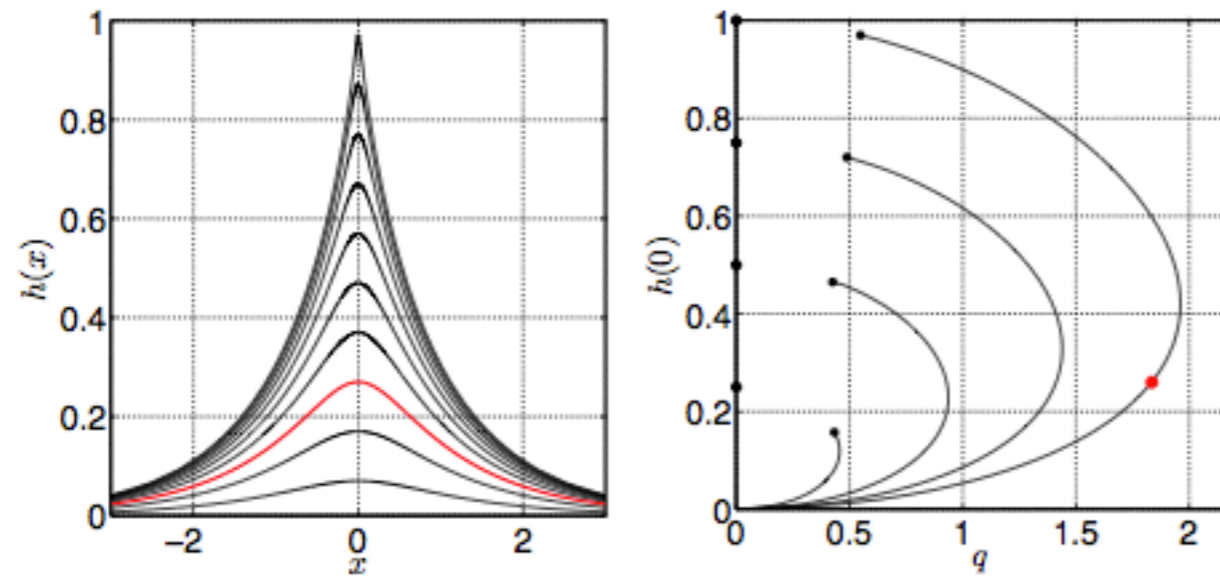
Solutions for modified problem, forced by a dipole:



$\rho=1$, dipole forcing

Pressure balances for modified problem, forced by a dipole:





Left: computed solutions with $l = 1$, $M = 256$.

Right: q - $h(0)$ bifurcation diagrams for $l \in \{0.25, 0.5, 0.75, 1\}$.

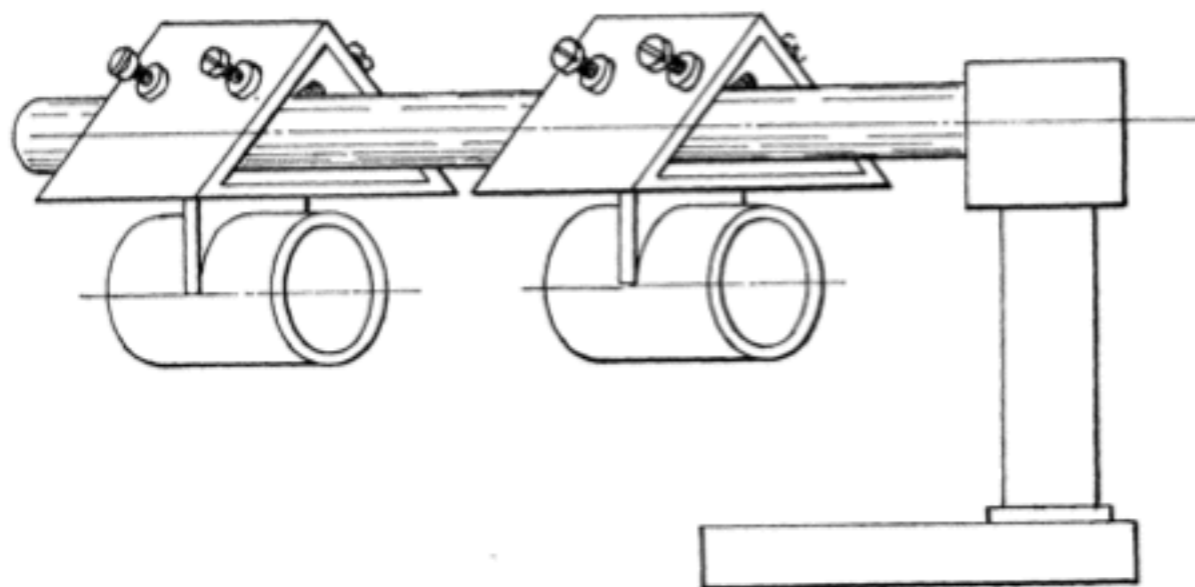
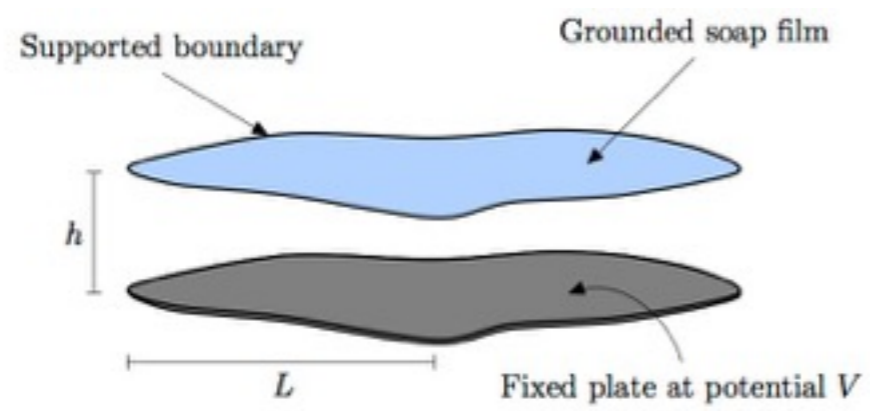


FIGURE 2. Apparatus for holding two circular soap films in position.

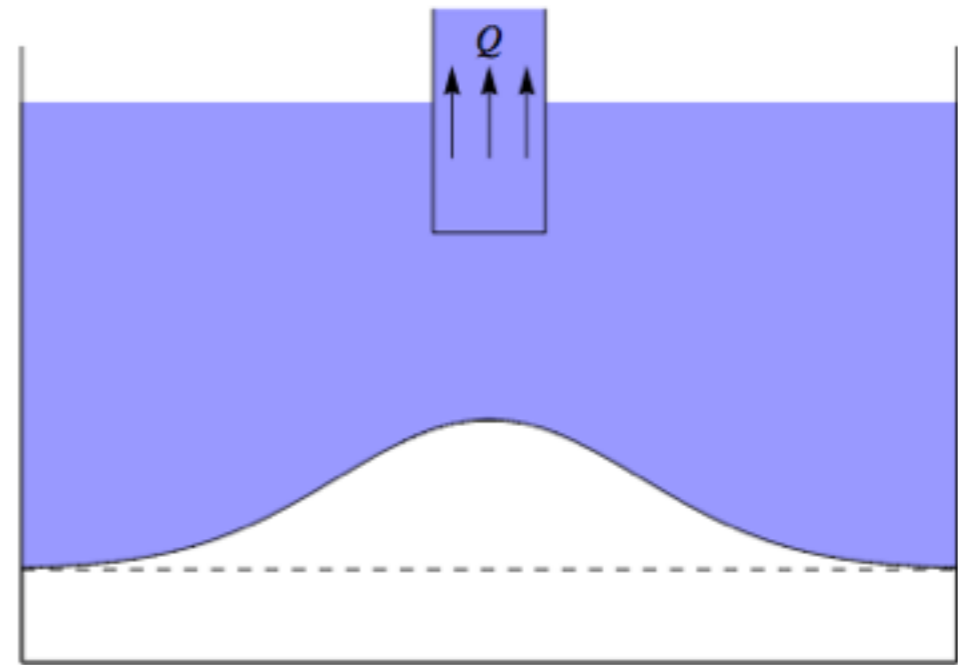


Selective Withdrawal

- ▶ Two deep layers of immiscible fluids.
- ▶ Fluid from the upper layer is withdrawn at a constant rate Q .



Initial configuration

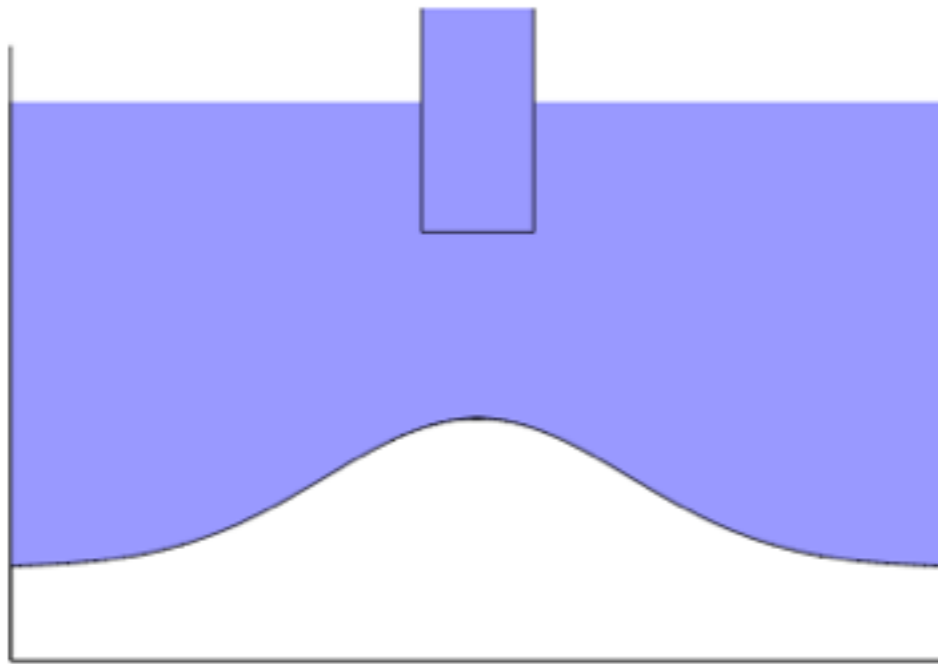


Steady-state selective withdrawal

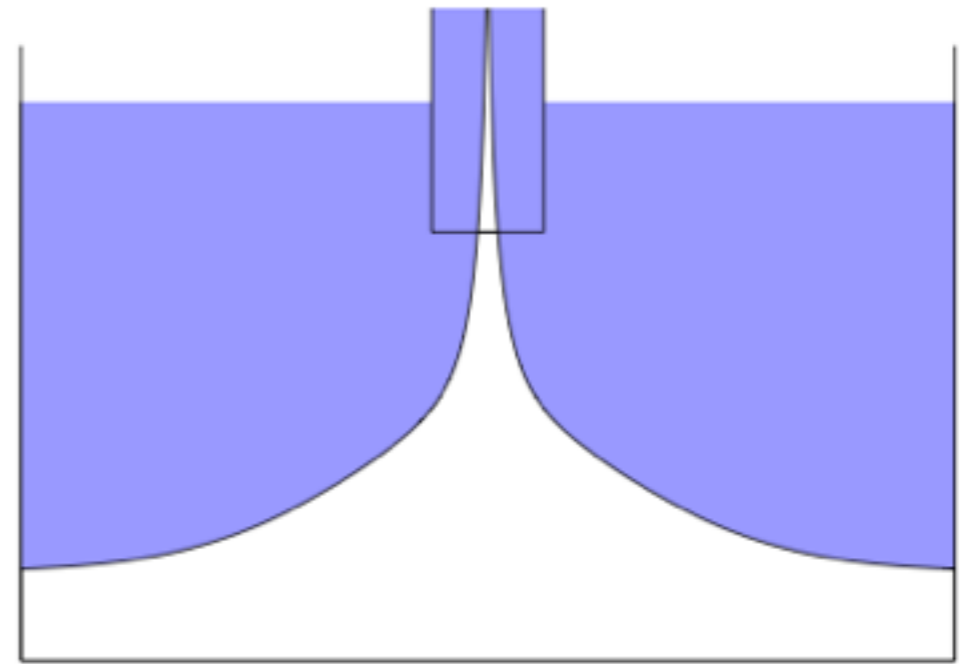
The resulting *steady-state* flows are studied.

Topological transition

There are two distinct classes of steady-states in such systems:



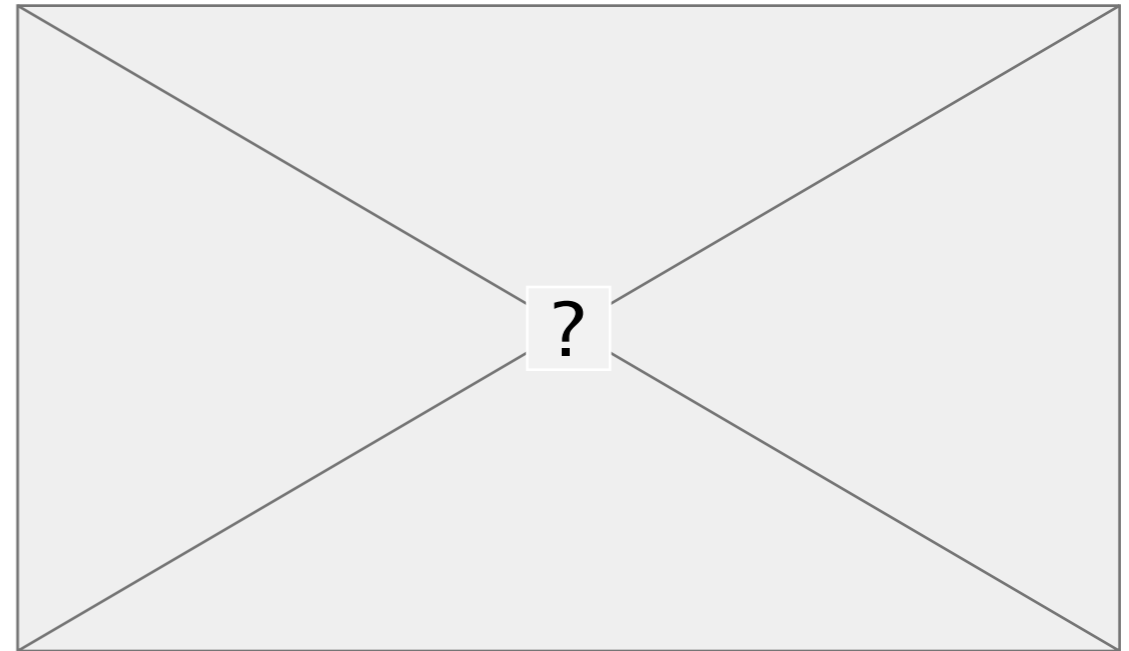
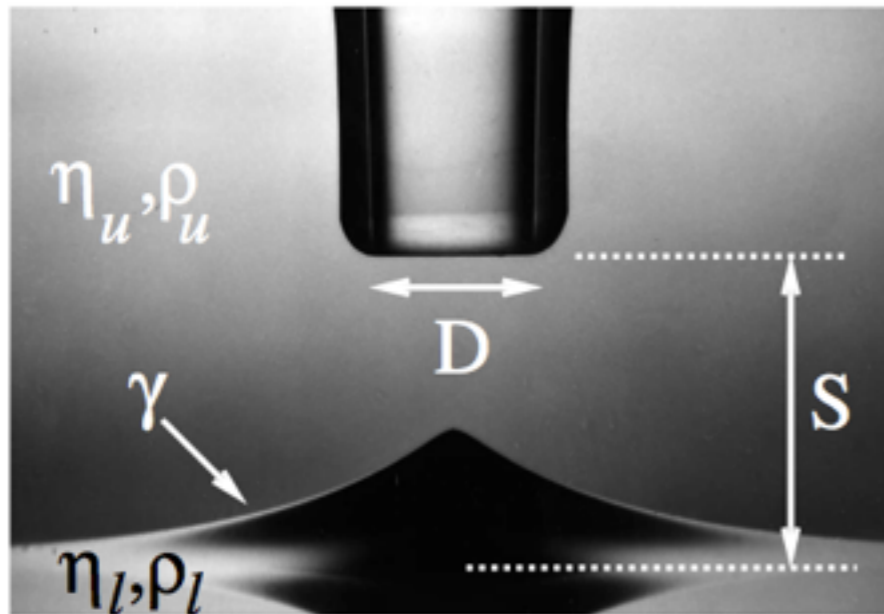
Selective withdrawal (*hump*)



Viscous entrainment (*spout*)

Low Q $\xrightarrow{\text{Transition (through steady states)}}$ High Q

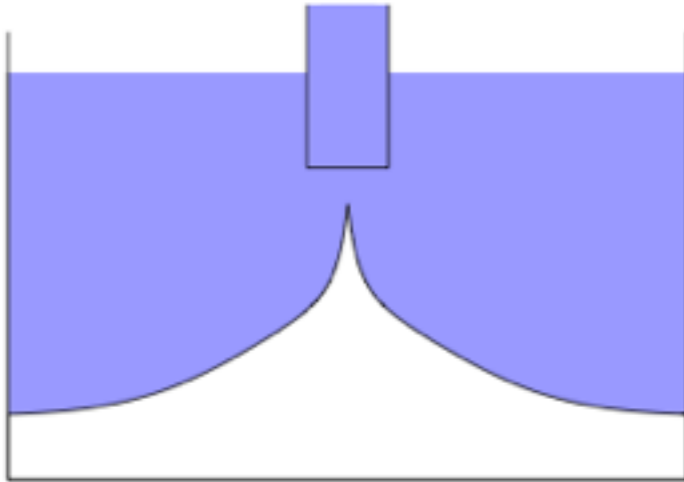
Continuous bifurcation?



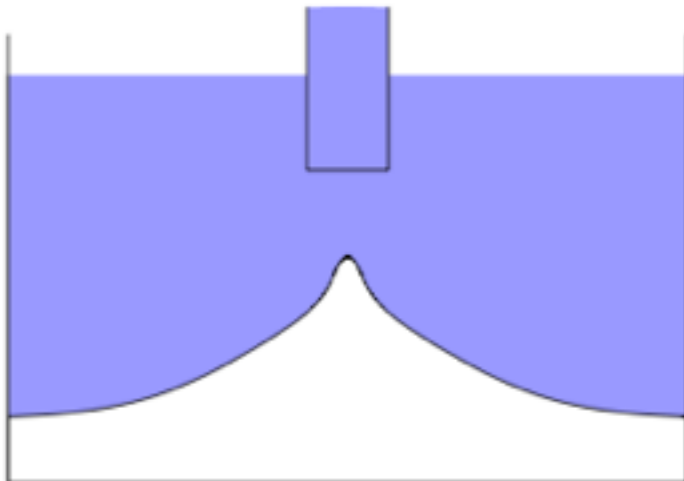
$$W \propto (Q - Q_c)^\gamma$$

I. Cohen and S. R. Nagel, Phys. Rev. Lett. 88, 074501 (2002)

Regularity of the interface

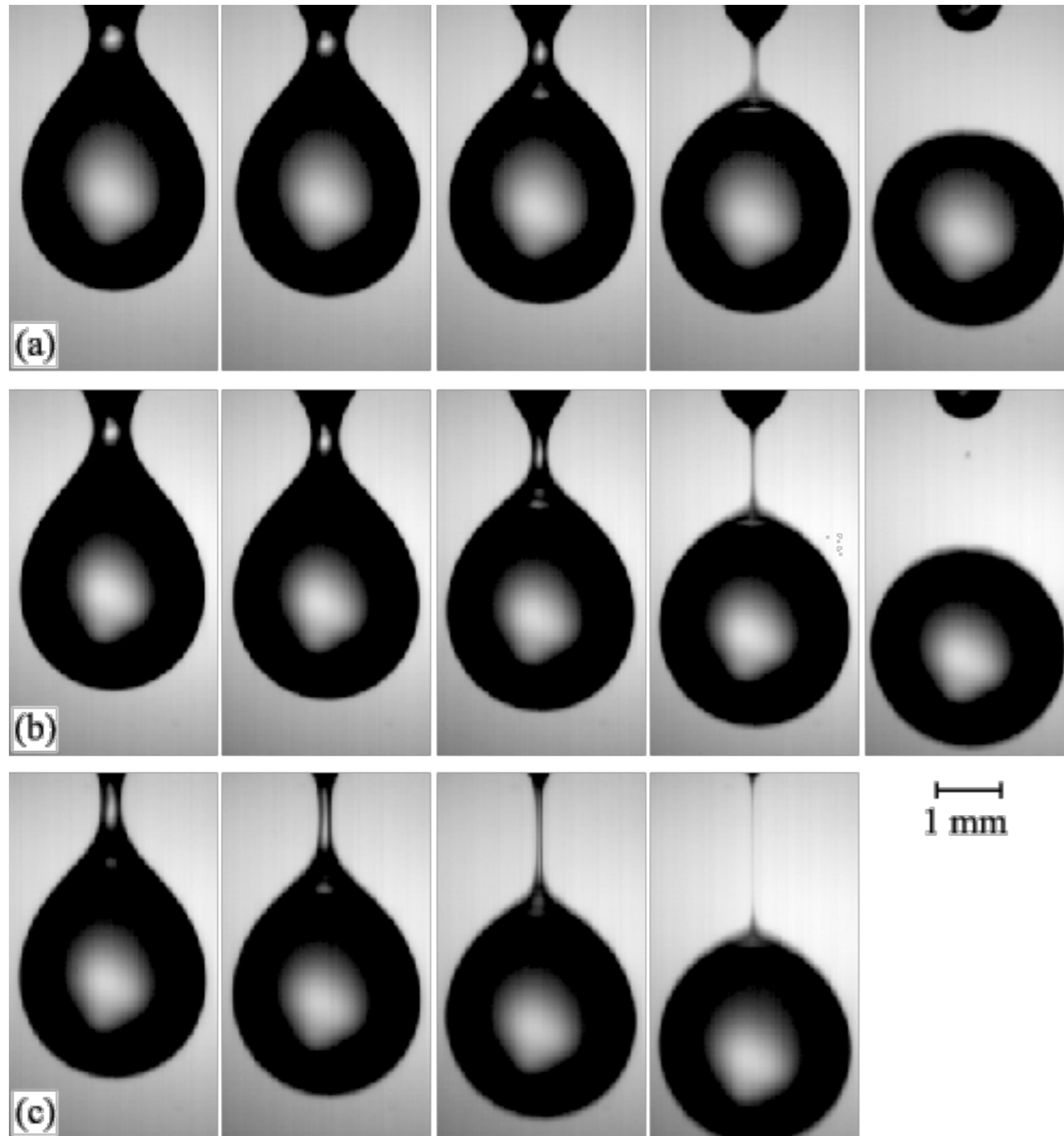


Does the interface become singular?



If not, which parameters control the cutoff length scale?

Dynamics vs static singularities

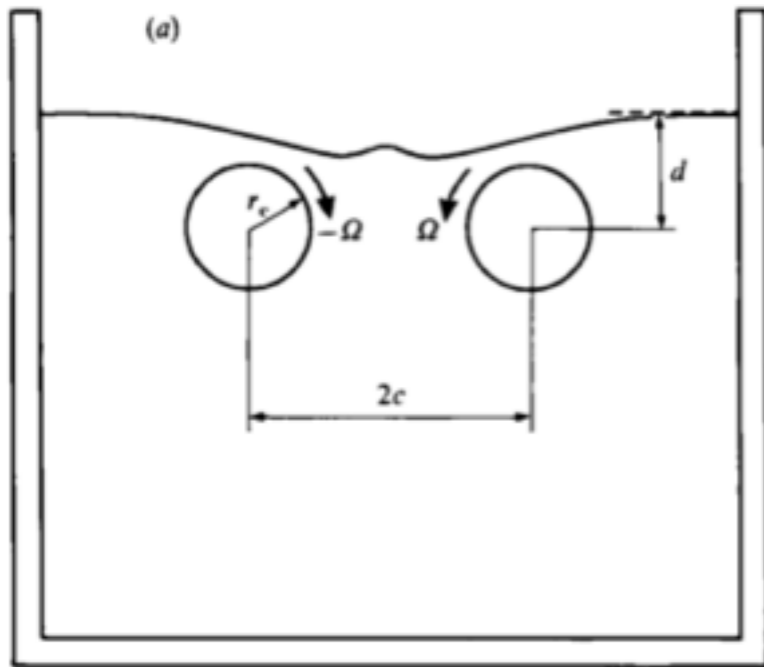


Folklore "Theorem":

For slow flows,
Viscous + Capillary
Forces = No steady
state singularities

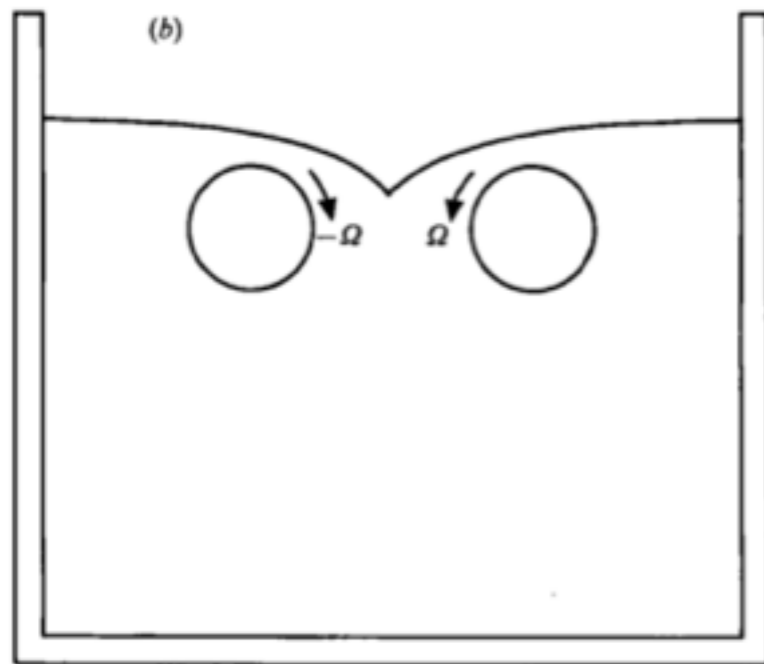
Alexander Rothert, Reinhard Richter and Ingo Rehberg,
New J. Phys. 5 (2003) 59

Selective Withdrawal in 2D



$$Ca \approx \frac{\mu}{\sigma} \Omega d$$

$$\frac{R}{d} \sim \exp(-Ca)$$



Exponentially sharp cusps!

J. Fluid Mech. (1992), vol. 241, pp. 1-22
Printed in Great Britain

**Free-surface cusps associated with flow at low
Reynolds number**

By JAE-TACK JEONG† AND H. K. MOFFATT

2D free surface cusps

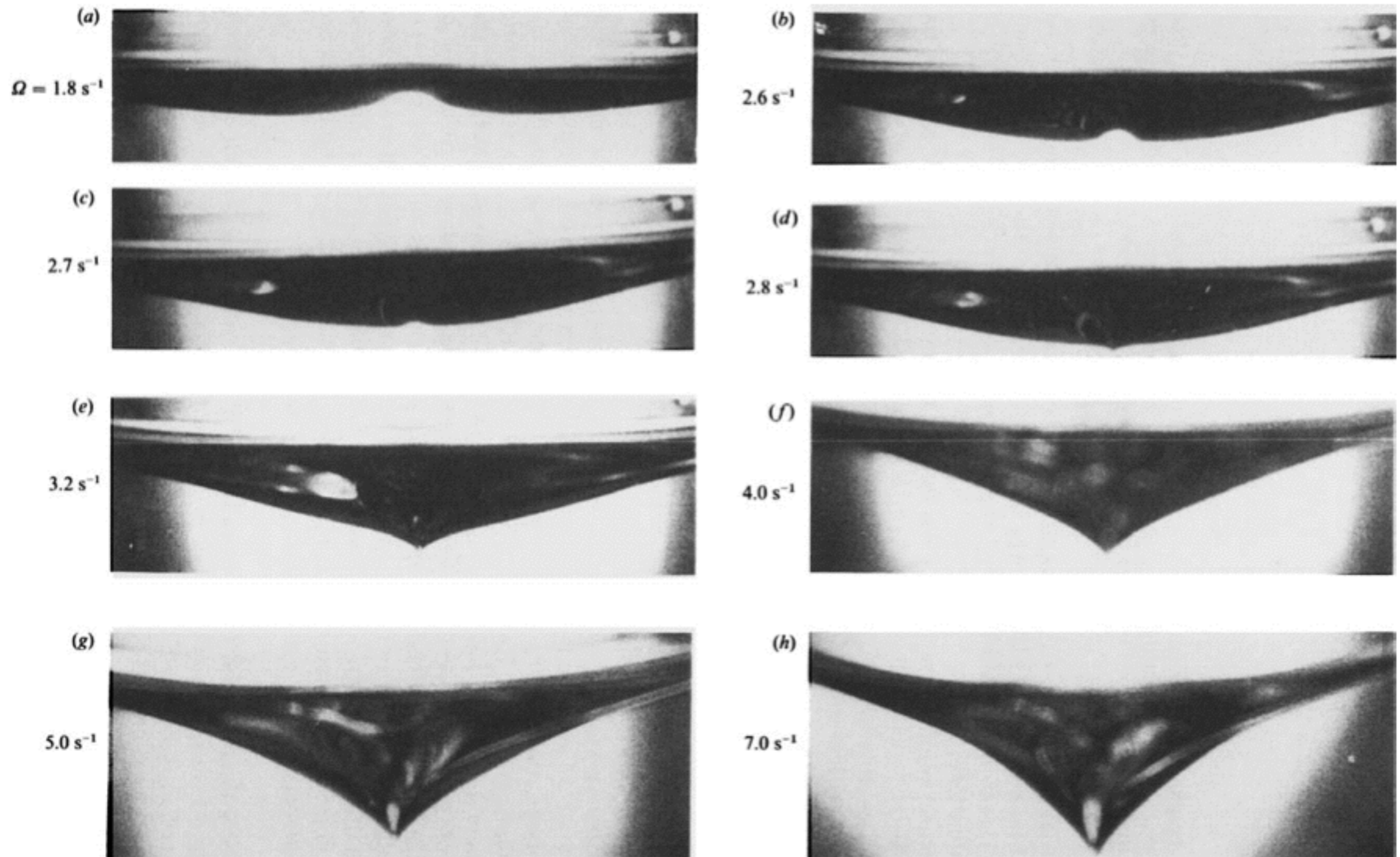
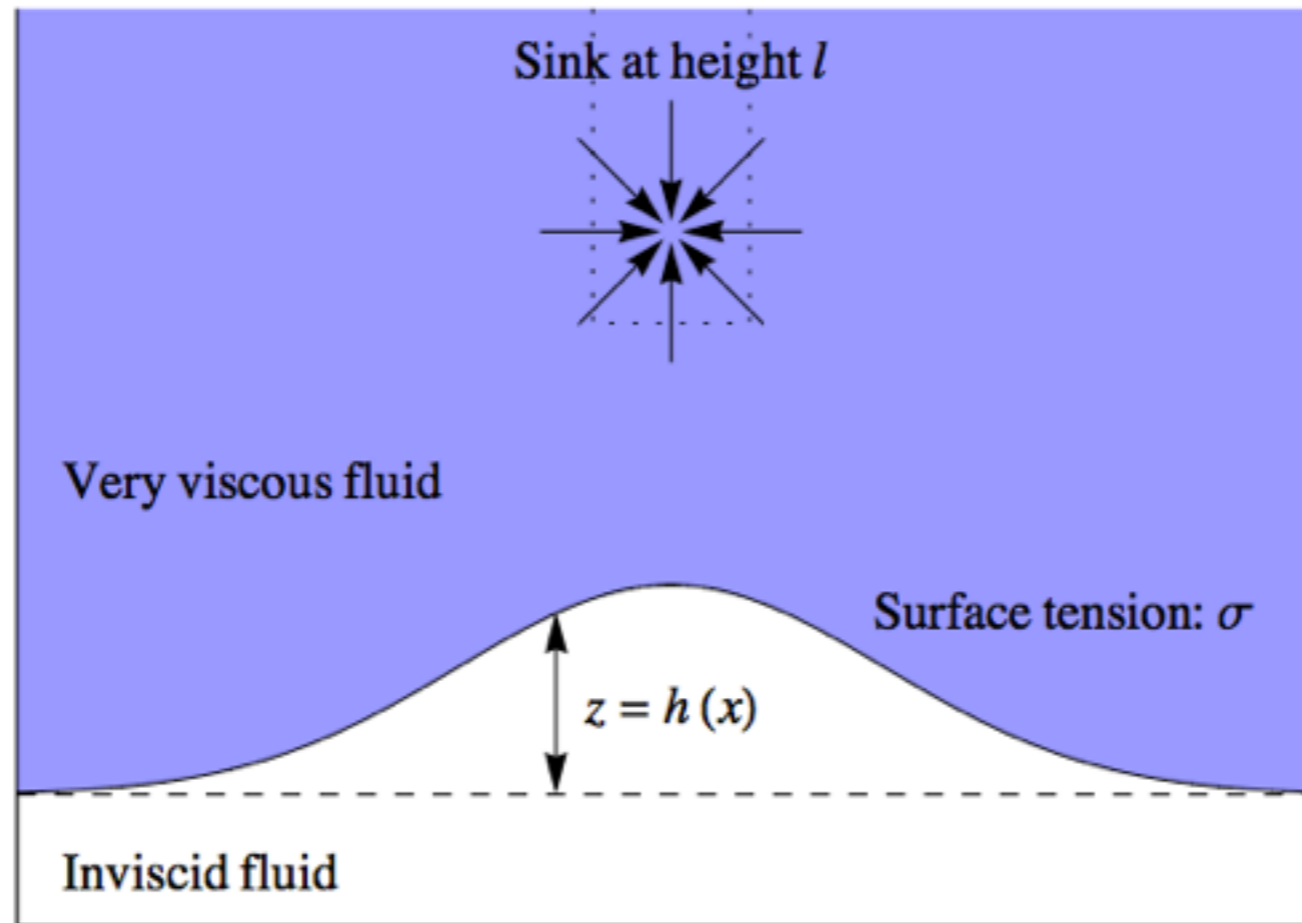


FIGURE 13. Sequence of photographs showing the transition from crest to cusp as Ω is increased through a critical value $\Omega_c \approx 2.75 \text{ s}^{-1}$. The capillary number $\mathcal{C}_{\text{exp}} = \mu\Omega r_c/\gamma$ has the following values: (a) 15.7; (b) 22.7; (c) 23.6; (d) 24.4; (e) 27.9; (f) 34.9; (g) 43.6; (h) 61.1. The horizontal extent of the free surface shown in each of these photographs is approximately 5 cm.

Modeling Selective Withdrawal

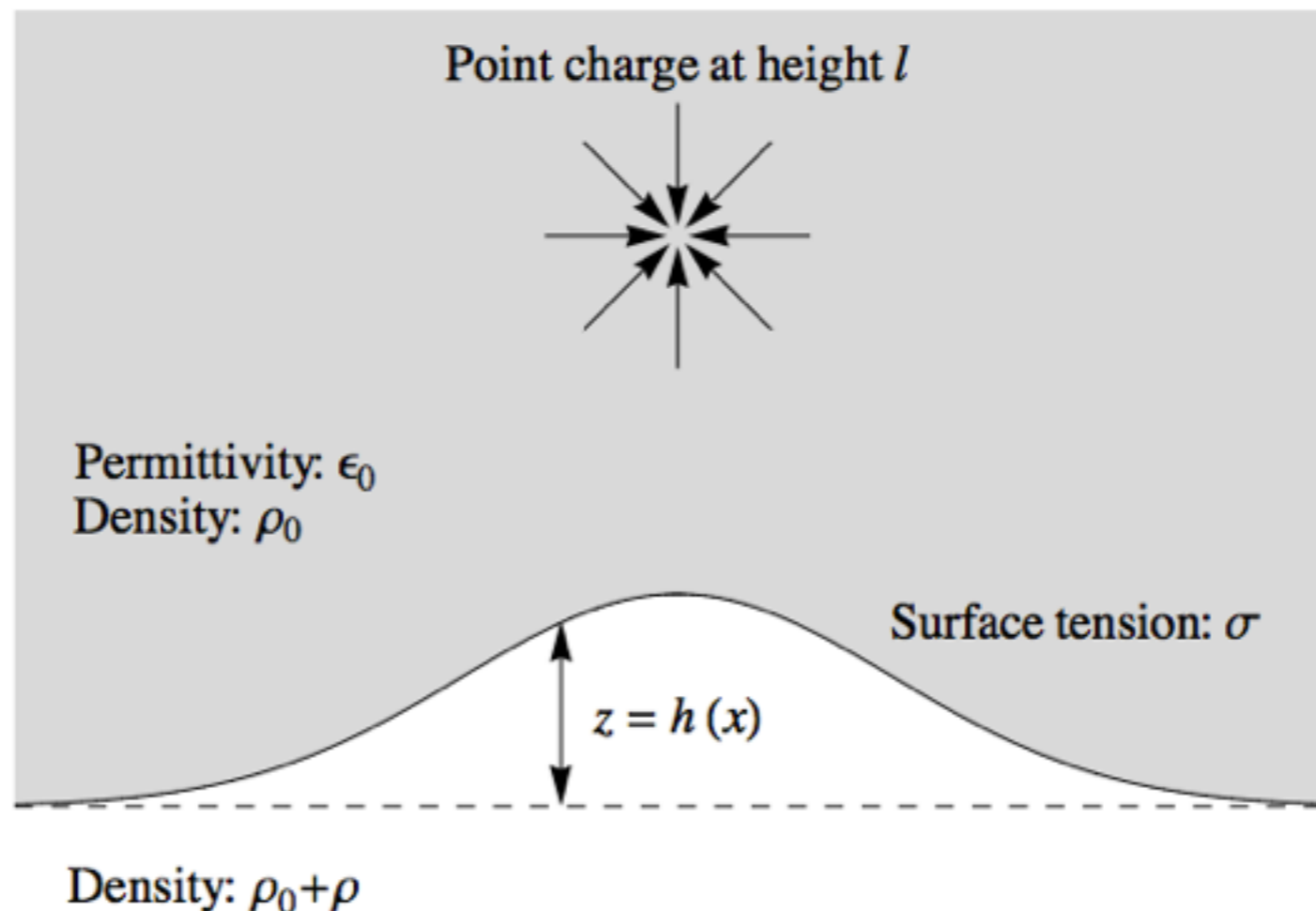


- ▶ The upper fluid ($z > h$) has density ρ_0 and is very viscous.
- ▶ The lower fluid ($z < h$) has density $\rho_0 + \rho$ and is inviscid.
- ▶ The withdrawal flow is equivalent to a point sink.

Electro-mechanical analogue

Electrostatic Analogy: *captures the essential features of the fluids problem in a setting where analysis is simpler.*

- ▶ Point sink \rightarrow point charge.
- ▶ Velocity field $u^{(h)}$ \rightarrow electrostatic potential ϕ .
- ▶ Fluid interface \rightarrow conducting elastic sheet.



Discretization: FFT

Discretization: FFT

We compute (FFT) coefficients C_n such that

$$\sum_{n=-M+1}^M C_n e^{in\theta_j} = h_j + 0i, \quad j = -M+1, \dots, M$$

then ‘apply’ the discrete Hilbert transform:

$$\mathbb{B}_n = \begin{cases} C_0, & n = 0, \\ C_M, & n = M, \\ 2C_n, & n = 1, \dots, M-1, \\ 0, & n = -(M-1), \dots, -1. \end{cases}$$

Finite dimensional representation

Discrete Analytic functions

The function

$$F(w) = \sum_{n=-M+1}^M \mathbb{B}_n w^n = \sum_{n=0}^M \mathbb{B}_n w^n$$

is analytic in \mathbb{D} and satisfies $\operatorname{Re}(F(e^{i\theta_j})) = h_j$ at each node $e^{i\theta_j}$.

We combine this map with a “stretching” term to create the full family of maps studied.

Collocation Method

Collocation Method

We seek the best fit solution of the form

$$\mathbb{F}(w) = \underbrace{\mathbb{A} \left(\frac{1-w}{1+w} \right)}_{\text{stretch}} + \underbrace{\sum_{n=0}^M \mathbb{B}_n w^n}_{\text{deflection}}$$

with

$$\mathbb{F}(0) = l,$$

$$\mathbb{F}(1) = h(0),$$

$$\mathbb{F}(\bar{w}) = \overline{\mathbb{F}(w)},$$

$$\sum_{n=0}^M \mathbb{B}_n (-1)^n = 0.$$

Collocation Method

Collocation Method

We seek the best fit solution of the form

$$\mathbb{F}(w) = \underbrace{\mathbb{A} \left(\frac{1-w}{1+w} \right)}_{\text{stretch}} + \underbrace{\sum_{n=0}^M \mathbb{B}_n w^n}_{\text{deflection}}$$

with

$$\mathbb{F}(0) = l,$$

$$\mathbb{F}(1) = h(0),$$

$$\mathbb{F}(\bar{w}) = \overline{\mathbb{F}(w)},$$

$$\sum_{n=0}^M \mathbb{B}_n (-1)^n = 0.$$

Collocation Method

Collocation Method

We seek the best fit solution of the form

$$\mathbb{F}(w) = \underbrace{\mathbb{A} \left(\frac{1-w}{1+w} \right)}_{\text{stretch}} + \underbrace{\sum_{n=0}^M \mathbb{B}_n w^n}_{\text{deflection}}$$

with

$$\mathbb{F}(0) = l,$$

$$\mathbb{F}(1) = h(0),$$

$$\mathbb{F}(\bar{w}) = \overline{\mathbb{F}(w)},$$

$$\sum_{n=0}^M \mathbb{B}_n (-1)^n = 0.$$

Collocation Method

Collocation Method

We seek the best fit solution of the form

$$\mathbb{F}(w) = \underbrace{\mathbb{A} \left(\frac{1-w}{1+w} \right)}_{\text{stretch}} + \underbrace{\sum_{n=0}^M \mathbb{B}_n w^n}_{\text{deflection}}$$

with

$$\mathbb{F}(0) = l,$$

$$\mathbb{F}(1) = h(0),$$

$$\mathbb{F}(\bar{w}) = \overline{\mathbb{F}(w)},$$

$$\sum_{n=0}^M \mathbb{B}_n (-1)^n = 0.$$

Collocation Method

Collocation Method

We seek the best fit solution of the form

$$\mathbb{F}(w) = \underbrace{\mathbb{A} \left(\frac{1-w}{1+w} \right)}_{\text{stretch}} + \underbrace{\sum_{n=0}^M \mathbb{B}_n w^n}_{\text{deflection}}$$

with

$$\mathbb{F}(0) = l,$$

$$\mathbb{F}(1) = h(0),$$

$$\mathbb{F}(\bar{w}) = \overline{\mathbb{F}(w)},$$

$$\sum_{n=0}^M \mathbb{B}_n (-1)^n = 0.$$

Residual

Conjugate gradient minimization of residual

Even node spacing also allows efficient evaluation of the residual pressure

$$\frac{\text{Im}(\zeta_{\theta\theta}(\theta)\overline{\zeta_{\theta}(\theta)})}{|\zeta_{\theta}(\theta)|^3} - \text{Im}(\zeta(\theta)) - \left(\frac{q}{2\pi|\zeta_{\theta}(\theta)|}\right)^2$$

via the FFT.

Example:

$$\zeta(\theta_j) = \mathbb{G}(e^{i\theta_j}) = \mathbb{A} \left(\frac{1 - e^{i\theta_j}}{1 + e^{i\theta_j}} \right) + \sum_{n=0}^M \mathbb{B}_n e^{in\theta_j}$$

